




Review

A Comprehensive State-of-the-Art Review on the Recent Developments in Greenhouse Drying

Asim Ahmad ¹, Om Prakash ², Anil Kumar ³, Rajeshwari Chatterjee ⁴, Shubham Sharma ^{5,6,*}, Vineet Kumar ⁷, Kushagra Kulshreshtha ⁸, Changhe Li ⁶ and Elsayed Mohamed Tag Eldin ^{9,*}

- ¹ Faculty of Engineering and Applied Sciences, Usha Martin University, Ranchi 835103, India
² Department of Mechanical Engineering, Birla Institute of Technology, Mesra, Ranchi 835215, India
³ Department of Mechanical Engineering, Delhi Technological University, New Delhi 110042, India
⁴ Department of Hotel Management and Catering Technology, Birla Institute of Technology, Mesra, Ranchi 835215, India
⁵ Mechanical Engineering Department, University Center for Research & Development, Chandigarh University, Mohali 140413, India
⁶ School of Mechanical and Automotive Engineering, Qingdao University of Technology, Qingdao 266520, China
⁷ Department of Automobile Engineering, Chandigarh University, Mohali 140413, India
⁸ Institute of Business Management, GLA University, Mathura 281406, India
⁹ Faculty of Engineering and Technology, Future University in Egypt, New Cairo 11835, Egypt
* Correspondence: shubham.t1707@cumail.in or shubham543sharma@gmail.com or shubhamsharmacsircr@gmail.com (S.S.); elsayed.tageldin@fue.edu.eg (E.M.T.E.)

Abstract: Drying via solar energy is an environmentally friendly and inexpensive process. For controlled and bulk level drying, a greenhouse solar dryer is the most suitable controlled level solar dryer. The efficiency of a solar greenhouse dryer can be increased by using thermal storage. The agricultural products dried in greenhouses are reported to be of a higher quality than those dried in the sun because they are shielded from dust, rain, insects, birds, and animals. The heat storage-based greenhouse was found to be superior for drying of all types of crops in comparison to a normal greenhouse dryer, as it provides constant heat throughout the drying process. Hence, this can be used in rural areas by farmers and small-scale industrialists, and with minor modifications, it can be used anywhere in the world. This article provides a comprehensive analysis of the development of solar greenhouse dryers for drying various agricultural products, including their design, thermal modelling methods, cost, energy, and environmental implications. Furthermore, the choice and application of solar photovoltaic panels and thermal energy storage units in the solar greenhouse dryers are examined in detail, with a view to achieving continuous and grid-independent drying. The energy requirements of various greenhouse dryer configurations/shapes are compared. Thermodynamic and thermal modelling research that reported on the performance prediction of solar greenhouse dryers, and drying kinetics studies on various agricultural products, has been compiled in this study.

Keywords: greenhouse dryer; thermal storage; no-load condition; load condition; embodied energy; thermal modelling



Citation: Ahmad, A.; Prakash, O.; Kumar, A.; Chatterjee, R.; Sharma, S.; Kumar, V.; Kulshreshtha, K.; Li, C.; Eldin, E.M.T. A Comprehensive State-of-the-Art Review on the Recent Developments in Greenhouse Drying. *Energies* **2022**, *15*, 9493. <https://doi.org/10.3390/en15249493>

Academic Editor: Lyes Bennamoun

Received: 8 September 2022

Accepted: 18 November 2022

Published: 14 December 2022

Publisher's Note: MDPI stays neutral with regard to jurisdictional claims in published maps and institutional affiliations.



Copyright: © 2022 by the authors. Licensee MDPI, Basel, Switzerland. This article is an open access article distributed under the terms and conditions of the Creative Commons Attribution (CC BY) license (<https://creativecommons.org/licenses/by/4.0/>).

1. Introduction

Globally, in 2018–2019, fruit production was estimated to be 392 million tons, and vegetable production was estimated to be 486 million tons. Due to post-crop or post-harvest handling, nearly 30–40% agricultural produce is damaged or spoiled [1]. Among developing countries, India is the second-largest producer of vegetables and fruits; however, 35% of the crop is nevertheless lost post-harvest. The factors responsible for these losses include improper handling, poor production methods, and inadequate storage facilities. This results in the approximate annual financial loss of 104 million US dollars [2]. Spoilage

mainly occurs due to microorganisms, as a high percentage of water is present in fruits and vegetables.

To keep the agricultural product preserved, the removal of moisture content is essential. The most economical process of food preservation involves drying foodstuffs in the sun, a method which has been practiced for 5000 years. The dehydration of agricultural products takes place due to heat treatment, either via a natural or artificial process. The heat can be generated via a natural method, such as solar radiation, or via an artificial method, such as the generation of electricity by burning fossil fuels. The entire world faces the issue of an energy crisis due to the limited availability of fossil fuels and the rapid increase in the consumption of oil and natural gas. Electricity is either unavailable to many farmers or too expensive. Moreover, the supply of electricity is exceptionally erratic; therefore, dependence on its supply is an unreliable prospect for many farmers. To run the farm machinery on fossil fuels, on a large scale, is not financially prudent and it can significantly impede the management of the farm [3].

One of the most important and all-encompassing phenomena is global warming, as it affects flora and fauna across the globe. The diverse ways in which humans are broadly affected by global warming include rises in air temperature, rises in sea level, and changes in climate. These disturbances occur due to the high melting rates of snow/ice, the distinct differences in geographical distribution norms, and the extinction of animals and plants. The environmental system is degrading due to the ill effects of greenhouse gases [4].

The weather pattern is therefore affected. There is an uneven distribution of rain, and some parts of the world are left dry and arid. Renewable energy sources are the ultimate solution to deal with these unavoidable problems. The sun is the ultimate source of renewable energy, and it is the best renewable energy source to capitalize upon. Solar concentrators, solar collectors, and solar dryers utilize solar radiations for drying applications; farmers and small stakeholders find these to be the most flexible options for obtaining energy [5].

1.1. Solar Drying

Since ancient times, the solar drying method has been used by mankind to dry fruits, seeds, plants, wood, meat, fish, and other agricultural and animal products. The sun provides a free and renewable energy source for drying purposes. Several scientific research methods have been applied in order to improve solar dryers for the preservation of forest and agricultural products. Solar radiation is used to evaporate the moisture that is present in the product during the natural sun drying process; nevertheless, there is seasonal variation with regard to the intensity of sunshine, which can cause uneven drying, thus resulting in the under-drying and over-drying of products [6]. Solar energy is used to heat the air, and this heated air is able to flow over the product, thereby removing the moisture and carrying away the vapor released from the product. The equipment that harnesses the solar energy to heat the air and dry the food products has acquired the term, "Solar Dryer". The solar dryer mitigates the limitations of natural sun drying by improving the quality of the dried product. During the solar drying process, solar energy is used as the only energy source, or it is augmented by adding hybrid energy sources. Natural or forced convection airflow can be generated by the solar dryer [7].

During the drying process, the product may be subjected to preheated air as a result of convection, or the product may be directly exposed to heat due to solar radiation. The vaporization of moisture occurs as a result of the heat being absorbed by the agricultural product. Moisture is vaporized from the moist surface of the product when the heat is absorbed. This vaporization increases the temperature of the agricultural product, which results in the enhancement of the agricultural product's vapor pressure in comparison with the surrounding air. The ability of moisture to diffuse into the crop's surface from the interior depends on the size of the product, the moisture content, and the nature of the product. Solar drying usually occurs when agricultural products are available in abundance. Solar drying technologies provide an opportunity to sell dried products during off-season

periods. Moreover, the products can be sold at higher prices during harvesting seasons because of its superior quality.

There are various types of solar drying technologies, with each having their own merits and demerits. The use of the solar dryer depends upon the metrological conditions of the crop. The rate of drying inside the solar dryer is always higher in comparison with the drying rate in the sun. Additionally, the crops that are dried inside the solar dryer contain a higher amount of Vitamin A and Vitamin C. The solar dryer also minimizes crop losses that are caused by rain and dirt. The solar dryer is mainly categorized into three modes that are based on drying (i.e., open, direct, and indirect drying) [8].

1.1.1. Open Sun Drying

With open sun drying, the short wavelength of solar radiation descends on the rough surface of the agricultural crop. The surface absorbs part of the short wavelength radiation, depending on the color of the exposed crop, and the remaining part is diffused. There is an increase in the temperature of the crop due to the absorption of solar radiation as it converts solar radiation into thermal energy; this results in the loss of long-wavelength radiation from the surface of the agricultural product to the ambient surroundings through moist air.

Wind blowing over the surface of the crop also adds to the convective heat loss. The crop is dried as the evaporation of moisture takes place in the form of evaporative losses. Figure 1 illustrates the open-air drying process.

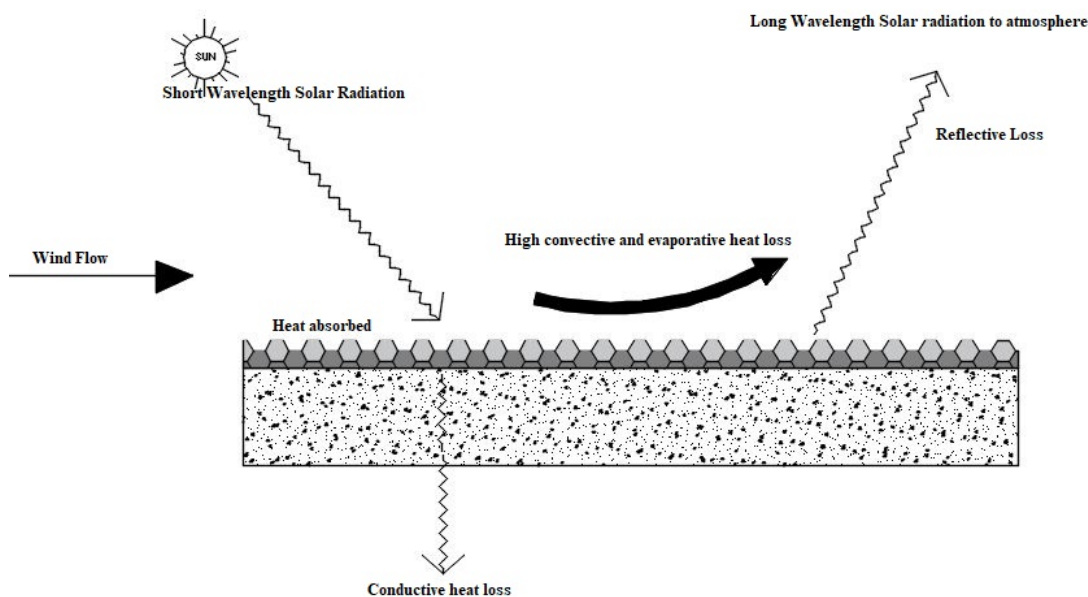


Figure 1. Open sun drying [9].

Open sun drying is the cheapest and simplest method of drying; however, many drawbacks are associated with this method. The prominent economic concern regarding this method is that open sun drying fails to maintain a standardized international quality, therefore, products obtained from this method remain out of the global market [10]. With the realization that the quality of the product obtained from open sun drying is deficient, a technically improved solar energy utilization method emerged; this is called solar or control drying [11].

1.1.2. Direct Solar Drying

Solar radiation incidents on the transparent glass cover are easily transmitted into the cabinet of the dryer. Most of the radiation is transmitted into the cabinet of the dryer, and the remaining part of the radiation is reflected back. The crop surface reflects part of the radiation, and the remaining part is absorbed by the crop surface, which thus increases the

temperature of the crop. The heated crop starts emitting long-wavelength radiation, but the long wavelength radiation cannot escape into the atmosphere due to the presence of the glass walls and cover; thus, the presence of both the incidental and reflected radiation within the chamber further increases the temperature to be higher than that of the crop [12]. Figure 2 illustrates a direct solar drying system.

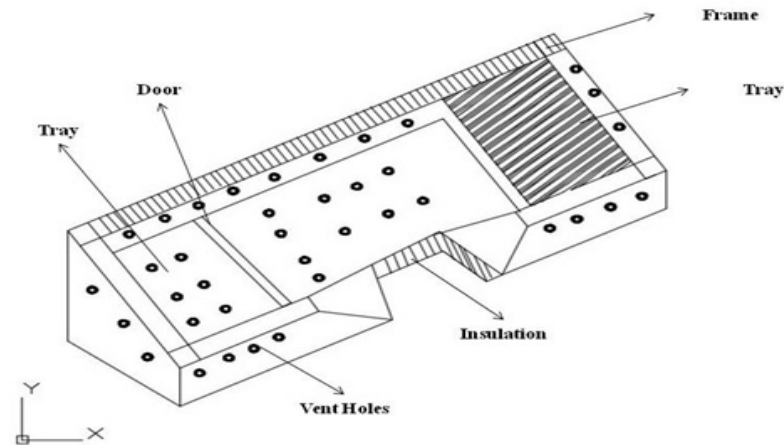


Figure 2. Direct solar drying [9].

1.1.3. Indirect Solar Drying

The indirect solar drying process occurs when the crops in drying chamber are not exposing to solar radiation. In the indirect solar dryer, a solar heater is used to dry the air, which is then passed through the drying chamber, either via natural or forced convection. The black painted absorption surface of the simple solar air heater absorbs the solar radiation and transmits it in the form of thermal energy (heat) to a working fluid [13]. Figure 3 represents an indirect solar drying system. The dryer's chamber is connected to an absorber panel. The temperature of the air that is present inside the drying chamber is increased due to the decrease in solar radiation on the flat plate collector; this heated air passes through the drying chamber via natural circulation or forced circulation. The airflow rate can be controlled (increased) by using a drying chamber with a chimney or by providing a wind operated ventilator situated on the upper portion of the chamber. To further regulate the temperature of the unit, a fueled heat source is also installed, along with an indirect solar dryer [14].

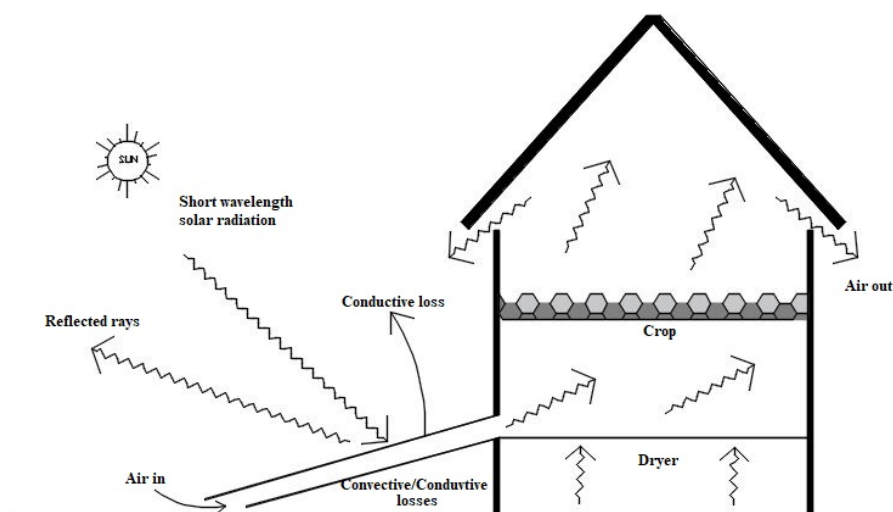


Figure 3. Indirect solar drying [9].

An assessment of the energy required for drying the agricultural products can be conducted using the initial and final moisture content for individual crops.

2. Greenhouse Dryer for Different Products

Using a greenhouse dryer is one way in which to conduct direct solar drying. The greenhouse effect is the underlying principle upon which the greenhouse drying system is based [15]. With regard to the greenhouse effect, the solar radiation received by the earth is trapped, thus increasing the overall temperature within the atmosphere. The atmosphere consists of gaseous matter and suspended particles, and it allows most of the incoming solar radiation to enter. The moment this radiation strikes the earth, part of it is immediately absorbed. Some of the energy is reflected back into the atmosphere, in the form of infrared rays, by the earth's surface [16]. Carbon dioxide (CO_2), water vapor, methane (CH_4), and nitrous oxide (N_2O) are the gases present in the atmosphere which absorb these infrared rays. The infrared rays that strike atmospheric particles are partially absorbed and partially redirected toward the earth; these rays are also absorbed. The greenhouse effect is the composite effect resulting from the earth's atmosphere absorbing infrared rays; this effect causes an increase in atmospheric temperature [17]. This natural phenomenon, where in heat is trapped by the earth's atmosphere, maintains a certain temperature range on earth in order to support life [18]. Figure 4 represents a greenhouse drying system.

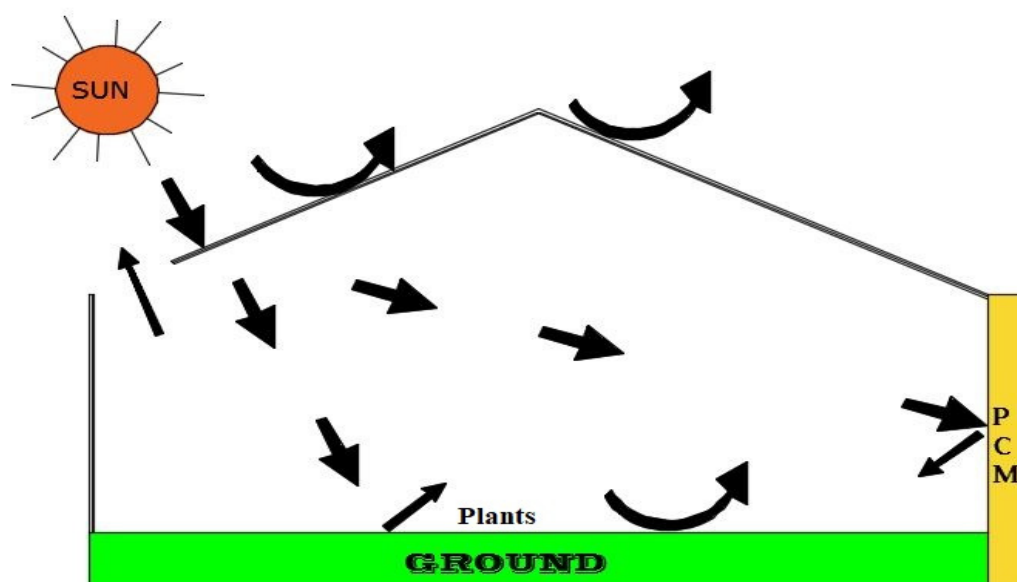


Figure 4. Greenhouse dryer with a PCM on the north wall [19].

The solar radiation consisting of short infrared wavelengths easily enters the transparent roof and walls of the dryer. It is partially absorbed by the object inside the dryer, which increases the temperature of the product. The heated object emits longer wavelengths, which is relative to its feeble intensity, and it is incapable of penetrating the transparent glass walls and rooves of the greenhouse [20]. The heat energy remains entrapped within the enclosure of the transparent glasshouse. This phenomenon, where in the temperature increases, is known as the greenhouse drying system, which is utilized for drying applications. It regulates the controlled environment; hence, it is also known as a controlled environment greenhouse [21].

2.1. Importance of Greenhouse Drying

The open sun drying technique is the most widely practiced method for the preservation of agricultural products in developing countries. This method does not provide satisfactory results under unfavorable weather conditions, and it can lead to the degradation of the quality and reliability of the product [22]. These losses mainly occur due to the

dust and dirt, as well as bacteria and insects. Alternative methods can avoid these losses by drying the agricultural products in a cheaper and more economical way. Using the greenhouse dryer could be the best alternative method to avoid the disadvantages of open sun drying [23].

In the GHD, crops are kept inside the trays in the enclosed structure, and the moisture removal process takes place either via a natural or forced convection mode. The mode of heat transfer depends on the removal of exhaust air from the dryer. The main advantages of using a GHD are:

- (i) The fabrication cost is low.
- (ii) The structure of a GHD can be used throughout the year, which helps to increase the production of a dried crop.
- (iii) Using a GHD improves the use of solar energy in terms of efficiency.

2.2. Greenhouse Dryers for Different Products

2.2.1. Red Chili

Khawale and Khawale (2016) conducted an experiment by using a solar dryer (double pass) when drying red chili. The results show that the average value of solar radiation is 566 W/m^2 and the air flow rate is 0.071 kg/s . The product moisture content was reduced from 80% to 9.1% by using a double pass indirect dryer. This process took 24 h, not including the evening hours. When the red chili was dried in the open sun, the process took 58 h. In this work, the collector efficiency and system drying efficiency were found to be 38% and 59.6%, respectively. The evaporative capacity of the system was observed to be in the range of $0.14\text{--}23 \text{ kg/h}$ [24].

Dhanore et al. (2014) evaluated the solar tunnel dryer's performance. This process was used for drying a sample of 5 kg of red chili. The moisture content was reduced to 5% from 75% during this process. The chamber and the ambient temperature were $51.68 \text{ }^\circ\text{C}$ and $39.1 \text{ }^\circ\text{C}$, respectively. The solar radiation ranged between 250 W/m^2 and 850 W/m^2 , and the air velocity was maintained at 0.5 m/s [25].

Fudholi et al. (2013) evaluated a red chili product being dried in both open sun and solar drying conditions. The drying performance of the product was observed during this process. The experimental results showed that the product dried in 30 h and the moisture content reduced from 80% to 10%. In open drying conditions, the product took 65 h to dry. In solar drying conditions, the time taken for the product to dry reduced by 49%. The average evaporation capacity and the average solar intensity were maintained at 0.97 kg/h and 420 W/m^2 , respectively. The Specific Moisture Extraction Rate (SMER) was observed to be 0.19 kg/kWh [26].

In Thailand, Kaewkiew et al. (2012) evaluated the drying of red chilis in a large-scale greenhouse solar dryer. The sheets in the dryer were made of polycarbonate and they were parabolically shaped. The concrete floor area was $8 \text{ m} \times 20 \text{ m}$, and nine D.C fans were installed for ventilation purposes. The moisture content of the red chilis was 74%, and they were dried in open dryer for three days. The solar radiation intensity during the drying process was observed as ranging between 390 W/m^2 and 820 W/m^2 . The color of the red chili was better maintained in the greenhouse dryer compared with the open sun dryer. The payback period of the large greenhouse dryer was found to be two years; this period must contend with numerous technical and economical parameters [27].

Banout et al. (2011) investigated the open, cabinet, and solar dryers (double pass) in terms of their performance when drying red chili. Regarding open sun drying, the process took 93 h; the process took 73 h in the cabinet dryer; and the process took 32 h in the double pass solar dryer. The chilis used had 10% moisture content. When compared with open sun and cabinet solar dryers, the solar dryer (double pass) has a higher ASTA (American Spice Trade Association) color value and low Vitamin C deterioration was observed. The construction cost of this dryer was greater compared with the cabinet dryer, but the drying rate per kg was less [28].

Mohanraj et al. (2009) evaluated the forced solar dryer design. The capacity of the dryer was 50 Kg, and it had graves for the heat storage of red chili. For 24 h, the red chili was dried, and the moisture content was reduced from 72.8 to 9.1%. The maximum solar intensity was observed to be 950 W/m^2 , and the average temperature in the dryer was $50.4 \text{ }^\circ\text{C}$. The efficiency of the dryer was found to be 21%. The specific moisture extraction rate was recorded at 0.87 Kg/kWh . The humidity was higher at the exit of the dryer, and it gradually decreased as the drying time increased, and at the final stage of the process, it became constant [29].

Hossain et al. (2013) examined are designed solar tunnel dryer, with a capacity of 80 kg, in order to dry fresh red chili. The drying time for the improved solar dryer was 20 h. It reduced the moisture content of the chili from 2.84 kg/kg to 0.04 kg/kg . Compared with the unimproved dryer, it took 32 h to reduce the moisture content from 0.41 kg/kg to 0.08 kg/kg . Green chili took 35 h to reduce the moisture content from 0.70 to 0.1 kg/kg using the traditional drying method; however, it took 22 h to reduce the moisture content from 7.5 kg/kg to 0.05 kg/kg using the improved dryer. Moreover, the quantity and pungency of the product can be improved, and the drying time can be reduced with blanching. The solar dryer's temperature was constant, and it recorded more than just the atmospheric temperature, which was $21.63 \text{ }^\circ\text{C}$. Blanching the red chili improved the color value [30].

2.2.2. Turmeric

Karthikeyan and Murugavelh (2018) worked on a mixed mode solar tunnel (forced convection). In order to harness the solar intensity effectively, inclination is the key factor. The moisture content was reduced from 0.779 kg/kg to 0.07 kg/kg of water/dry matter. The process of drying the product took 12 h compared with open sun drying, which took 43 h. The dryer's exegeric efficiency was found to be 48.11%, and energy utilization varies between 9.94% and 32.97%. Mathematical models were used in this experiment to observe the behavior of the turmeric [31].

Borah et al. (2015) designed and studied the performance of solar turmeric dryer. Inside the dryer, the temperature was found to be between 38 and $50 \text{ }^\circ\text{C}$, and the ambient temperature was recorded and found to be between 24 and $27 \text{ }^\circ\text{C}$. Both solid and sliced turmeric was used for the experiment, and the final moisture content was found to be between 6.37% and 15.49% for the solid turmeric, and 78.65% for the sliced turmeric after 12 h. The average effective moisture diffusivity was recorded to be $1.455 \times 10^{-10} \text{ m}^2/\text{s}$ for the solid turmeric and $1.852 \times 10^{-10} \text{ m}^2/\text{s}$ for the sliced turmeric. In each batch of turmeric powder, the curcumin content varied. During the heat processing of the turmeric, the curcumin content was found to be between 27 and 53%, and there was a maximum loss in pressure cooking for 10 min. The sliced turmeric drying rate was faster than the drying rate for the whole turmeric. For both the sliced turmeric and whole turmeric, the rates of drying were found to be similar, at 62%. Sliced turmeric requires a 25.5 h drying process. During the open sun drying process, the sliced turmeric is affected by white patches of fungal growth. When using a solar collective dryer, no fungal growth was observed, and a Page model was found to be effective for the analysis [32].

Gunasekar et al. (2020) investigated the performance of solar drying for drying turmeric. Biochemical constituents in turmeric, such as oleoresin, the total protein content of boiled turmeric, volatile oil, and curcuma, may vary. The quality of the turmeric may result in varying levels of moisture due to these biochemical constituents. Due to the boiling and drying processes of turmeric, the curcumin content was found to be intensified. During the open sun drying process, the drying time was 96 h, and it was 63 h during the solar drying process. The solar dryer temperature ranged between 28 and $88 \text{ }^\circ\text{C}$. The moisture content of turmeric was reduced from 79.04 to 7.14% over 12 days during the open sun drying process. The curcuma content varies non-linearly with respect to moisture content. Initially the moisture content in turmeric was found to be 2.89 g per 100 g at 78.04%, and it varied between 2.88 g and 4.55 g per 100 g sample during the open sun drying process.

A small variation in volatile oil content was shown during the open sun drying process. The volatile oil content before the drying process was found to be 5.9 mL/100 g of sample, after the drying process it was found to be 5.26 mL/100 g for the sun-dried sample, and it was 5.21 mL/100 g for the solar dried sample. The oleoresin content after the drying process was found to be 8.97 g/100 g of sample for the open sun drying process and it was 9.21 g/100 g of sample for the solar drying process. The boiled turmeric initially had oleoresin in content of 1.24 g/100 g of sample, and it also decreased linearly by 1.15 g/100 g of sample during the solar drying process, and by 1.77 g/100 g of sample during the sun drying process. By drying the product in a solar dryer, more proteins were obtained from the sun, and this is beneficial both biologically and theoretically [33].

Lakshmi et al. (2018) investigated the mixed mode solar dryer's (forced convective type) performance. This process is used for sliced turmeric samples that are integrated with the heat storage. In this process, 35 kg paraffin wax was used as the thermal storage during the liquid stage. The moisture level was reduced from 73.4 to 8.5% over 18.5 h in a mixed forced solar dryer, and in open sun drying conditions, it took 46.4 h. A moisture level of 12% was found after using the solar dryer, and when it was equipped with a solar air heater, the efficiency was calculated to be 25.6%. The mixed mode solar dryer saved time by 60%. The total flavonoids content for the solar dryer operating in a mixed mode was found to be 7.58 mg/g of sample, and it was found to be 1098 g and 8.08 g for fresh turmeric and solar dried turmeric, respectively. A high medical agriculture value was found after using the mixed mode solar dryer [34].

2.2.3. Copra

Yahya et al. (2018) evaluated the solar air dryer's (double pass) performance using a finned absorber for drying copra. During this drying process, the moisture level was reduced from 52.68 to 10.73% over 23 h, and in open sun drying conditions, it took 67 h. The air flow rate and the average rate of drying was maintained at 0.084 kg/s and 0.054 kg/h, respectively. For open drying and solar air drying, the average rate of drying was 0.191 kg/h. The efficiency of the system was found to be 39.47%, and the improved potential rate was 87.98 J. In Indonesia, open sun drying and smoke-drying processes are used for drying coconut; this has disadvantages such as debris, rain, and insect infestation [35].

Ayyappan et al. (2010) studied the copra drying process in a solar tunnel dryer. Under full load conditions, the natural conventional solar dryer took 57 h for the moisture content to reduce from 52.8 to 8%, and under half load conditions, it took 52 h. Compared with the open sun drying process (53%), good quality copra was obtained in the solar tunnel dryer (54.66%). The average efficiency was found to be 21%, and the solar intensity was found to be 860 W/m² [36].

Mohanraj et al. (2008) worked on a forced convective solar dryer, which involved designing, manufacturing, and testing it. Regarding its different levels, the moisture level was reduced from 51.8 to 7.8% on the bottom level, and it was reduced to 9.7% on the top level. The thermal efficiency of this system was found to be 24%. The kiln drying process was the alternative method to the open sun drying method for drying copra. In India, via direct contact with smoke, copra is dried, and the possibility for smoke deposition emerges. Copra with a high quality of 78% was achieved by using this dryer, and a thermal efficiency of 25% was achieved; the copra was left undamaged [37].

2.2.4. Grapes

The numerical model for the greenhouse solar drying of grapes was studied by Hamdi et al. (2018). The moisture level was reduced from 5.4 to 0.23 (g water/g dry matter) within 128 h. The temperature in the solar dryer was 55.98 °C compared with the ambient temperature that was found to be between 24.55 °C and 35.72 °C. The simulation of the mathematical model was conducted using TRNSYS software [38].

Ramos et al. (2015) developed a mathematical model based on the explicit finite difference. It was integrated with the heat and mass transfer model. The model incorporated

the effective moisture diffusivity parameter, which caused changes in terms of shrinkage and the reliance on thermal properties in water [39]. The simulation model predicted accurate times. The hemi cylindrical solar dryer's temperature was maintained between 55 and 80 °C. On the first day, the moisture content was reduced from 84% to 69%, and on the seventh day, it was further reduced to 16.5%. The pre-treatment process reduced the moisture content in less time [40].

Fadhel et al. (2005) revealed that greenhouse drying has zero running costs. The time taken to dry grapes in a solar greenhouse dryer, and via open sun drying, took 78, 120, and 205 h, respectively [41].

Yladiz et al. (2001) studied the regression model and estimated the coefficient and effect of an electric fan on air temperature. The moisture content in grapes was reduced to 0.15 kg water/kg of dry matter from 2.5–3.2 kg water/kg of dry matter. During the first 34 h of drying time, an air velocity of 1.0 m/s was recorded, and after 35 h, the air velocity was 1.5 m/s. The coefficient of regression and the R² was 0.98 and 4.10×10^{-3} , respectively [42].

2.2.5. Peanuts

Ester Y. Akoto et al. (2017) developed a solar dryer in order to improve peanut quality. The reduction in moisture content was 5.42% and 31.8% from 25.84% after single layer drying, and it was reduced to 4.24% after four layers drying, respectively [43].

The development of the dryer not only accelerated the drying of peanuts, thus enabling an evaluation of the quality of peanuts. Noomhorn et al. (1994) discovered that at 10 rpm, at a 75 °C temperature, and at a feed rate of 9 kg/min, the optimal quality was obtained. At higher temperatures, peanuts have poor quality index uniformity and a greater drying time because of the pressure of the sand. The drying time was reduced by reducing the feed rate and changing the rpm of the drum [44].

Bunn et al. (1972) studied an empirical equation related to high moisture content. It was tested in a drying environment, and it was also compared with frequently used drying methods [45].

2.2.6. Fish

Abdul Majid et al. (2015) experimented on 10 kg batch size solar dryer, studying silver cyprinid fish over 12 h. The moisture content was reduced to 18% from 72%, whereas in the open sun it took 20 h. The efficiency of the system and the collections were 12% and 9.4%, respectively. The bottom, middle, and top tray of the dryer maintained constant rate i.e., 0.145, 0.145, and 0.147 respectively [46].

Bassanio et al. (2011) designed the solar tunnel dryer to accommodate 50–110 kg. Half of the tunnel's base was used for drying and air heating for 30 h; the moisture content was reduced to 15.6% from 66.6%, and the efficiency of the dryer was 29.8%. The fish quality was enhanced in terms of flavor, food value, brightness, color, and taste [47].

Bhor et al. (2010) evaluated the solar tunnel dryer and found that the drying rate was higher compared with open sun drying. The temperature was maintained at 53.8 °C and the moisture content of the fish without salt was reduced to 19.04% over 33 h and 20% over 36 h for the upper and lower trays, respectively. In the case of sun drying, the moisture content reduced to 19.68% over 40 h. The salted fish's moisture content was reduced to 19.5% over 36 h and 19.6% over 38 h for the upper and lower trays, respectively [48].

3. Classification of the Greenhouse Drying System

There are three types of greenhouse dryers which are classified on the basis of air circulating within the drying chamber [49]:

- 3.1 Natural convection solar greenhouse dryer;
- 3.2 Forced convection solar greenhouse dryer;
- 3.3 Hybrid solar greenhouse dryer.

3.1. Natural Convection Solar Greenhouse Dryer

With this type of dryer, the incidental radiation is transmitted through the canopy of the system, which results in the heating of the crops. The temperature of the crop increases because solar radiation is absorbed. The principle of the thermosiphon effect works in the natural convection solar greenhouse dryer [50]. Ventilation is provided at the top of the dryer which enables humid air to be released from the dryer. The buoyant forces are responsible for the circulation of heated air through the crop when using this type of system. The movement of air within the drying chamber is called the passive mode and a dryer operating under such a convection mode of operation is termed as a natural convection solar greenhouse dryer [51]. Figure 5 shows the pictorial view of a natural convection solar greenhouse dryer.

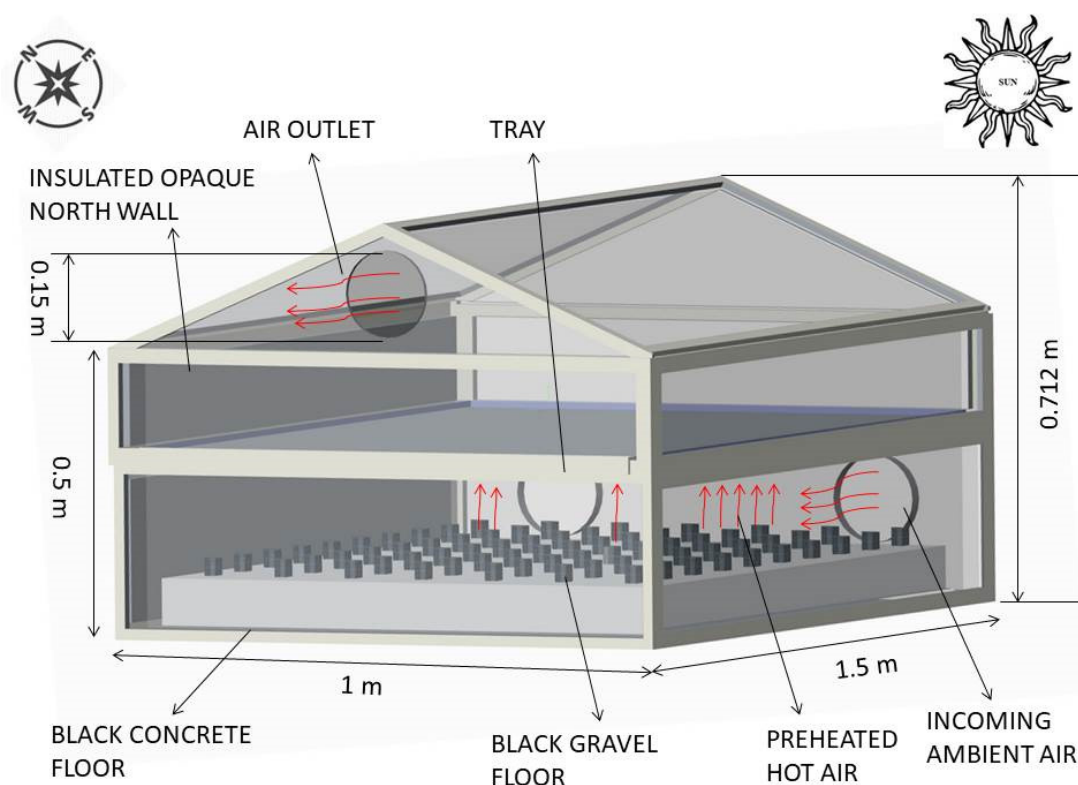


Figure 5. Pictorial view of a natural convection solar greenhouse dryer [52].

Natural circulation greenhouse dryers are used for drying agricultural products at the farm level because of the non-availability and erratic power supply in remote rural areas. It consists of an inclined collector coupled with a drying chamber, which contains trays to hold the agricultural products. The air circulation within the drying chamber takes place due to the differences in density; this occurs as a result of the buoyant forces [15].

However, due to high air resistance, airflow is not possible through the thin layer using natural convection; therefore, to increase the airflow, ventilators or chimneys are installed. Rodents and rain do not damage the dried products in the natural convection solar dryers during the drying process. Moreover, the drying time is minimized when compared with the open sun-drying process.

Natural circulation greenhouse dryers are modified forms of regular greenhouses. For a controlled airflow, vents of appropriate sizes and positions are incorporated into the dryer. The earliest types of passive solar greenhouse dryers are characterized by a large transparent cover of polyethene with an inclined glass roof to help allow direct solar radiation to cover the product [53]. The problems that arise from using natural convection greenhouse dryer include the holding capacity of the dryer, which results in low productivity; there is a risk of the air circulation failing, thus causing the drying products to spoil; and the exposure to

solar radiation may result in vitamin loss and decolorization. Ahmad and Prakash (2019) designed and built a greenhouse dryer that uses natural convection. The bed of the drying chamber was covered with sensible heat storage materials. Four distinct types of bed were chosen for the comparative heat transfer assessments of the proposed setup: a gravel bed, ground bed, concrete bed, and a black painted gravel bed. The black painted gravel bed provided conditions that produced the highest heat gain, which was 53%, whereas the corresponding values for the concrete bed, gravel bed, and ground bed were 33%, 49%, and 29%, respectively. As a result, a black-painted gravel bed is strongly advised for optimal heat storage [54]. From studying the literature, we may conclude that only forced ventilation systems containing a blower or a fan helps in the proper removal of moist air.

3.2. Forced Convection Greenhouse Dryer

In order to regulate the temperature and moisture evaporation, an optimum airflow is required for the greenhouse dryer throughout the drying process; this is achieved by observing the changes in the weather conditions [55]. An exhaust fan is installed on the west wall to eliminate the humid air [56]. The GHD airflow is regulated by the use of a blower or fan; this is called a forced convection solar greenhouse dryer [51]. Figure 6 shows the pictorial view of a forced convection solar greenhouse dryer.

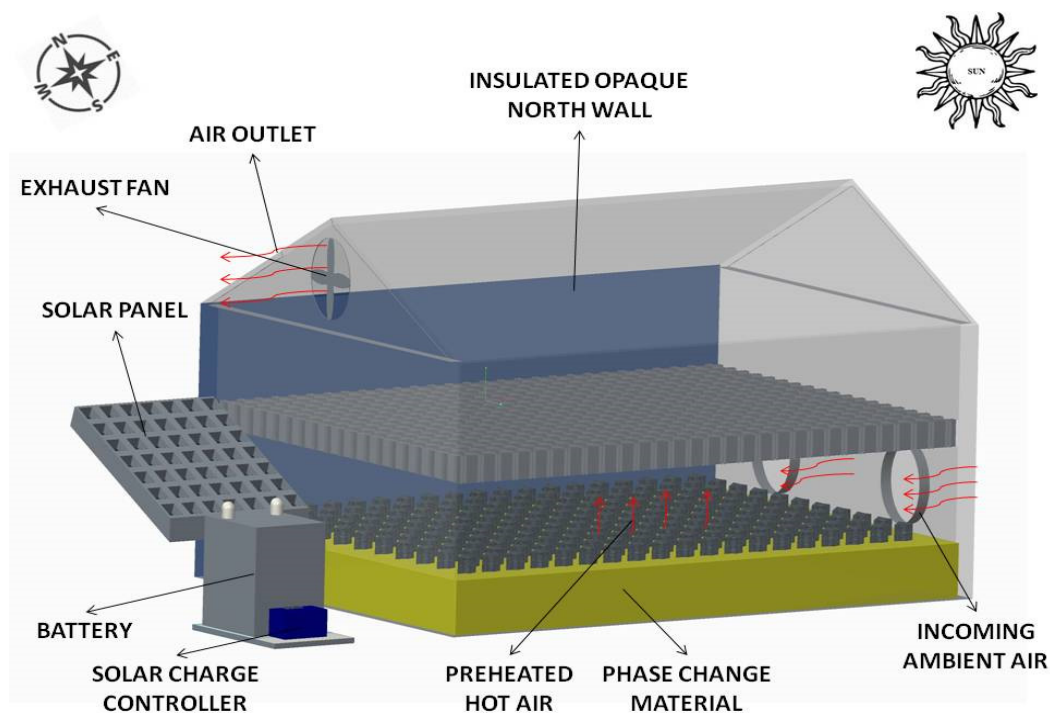


Figure 6. Forced convection solar greenhouse dryer.

Movement of the hot air from the drying chamber occurs as a result of the fans in the forced convection greenhouse dryers. For high moisture content products, such as tomatoes, papaya, grapes, chilis, kiwis, bitter-gourds, cabbages, brinjal, and cauliflower, forced convection greenhouse dryers are the most suitable [51].

The five basic components of a forced convection greenhouse drying system are: a drying chamber; a tray to contain the product that needs drying; an inlet hole; an outlet hole adjusted with a fan or blower for air circulation; and for a continuous steady power supply, a battery charging system is required. The heated air passing over the wet product facilitates moisture evaporation due to the convective heat transfer mode [57]. The difference in moisture concentration between the crop surface and dry air causes drying [58].

3.3. Solar Hybrid Greenhouse Dryer

The solar drying system is mainly divided into three modes of operation; direct mode, indirect mode, and hybrid mode. Regarding the hybrid solar dryer, the combination of two sources of energy is supplied for drying purposes. The combination of two sources can be wholly renewable or non-renewable [59]. The types of hybrid solar dryers are: (i) hybrid solar dryer assisted by geothermal energy; (ii) hybrid solar dryer assisted by biomass energy; (iii) hybrid solar dryer assisted by ocean/wind energy; (iv) hybrid solar dryer assisted by renewable energy; and (v) hybrid solar dryer assisted by solar air heater. In a hybrid greenhouse dryer, the dryer is assisted by other energy supplies [60]. Moreover, the hybrid dryer should have the ability to work in both an active and passive mode depending on what is required. Figure 7 represents the hybrid greenhouse dryer.

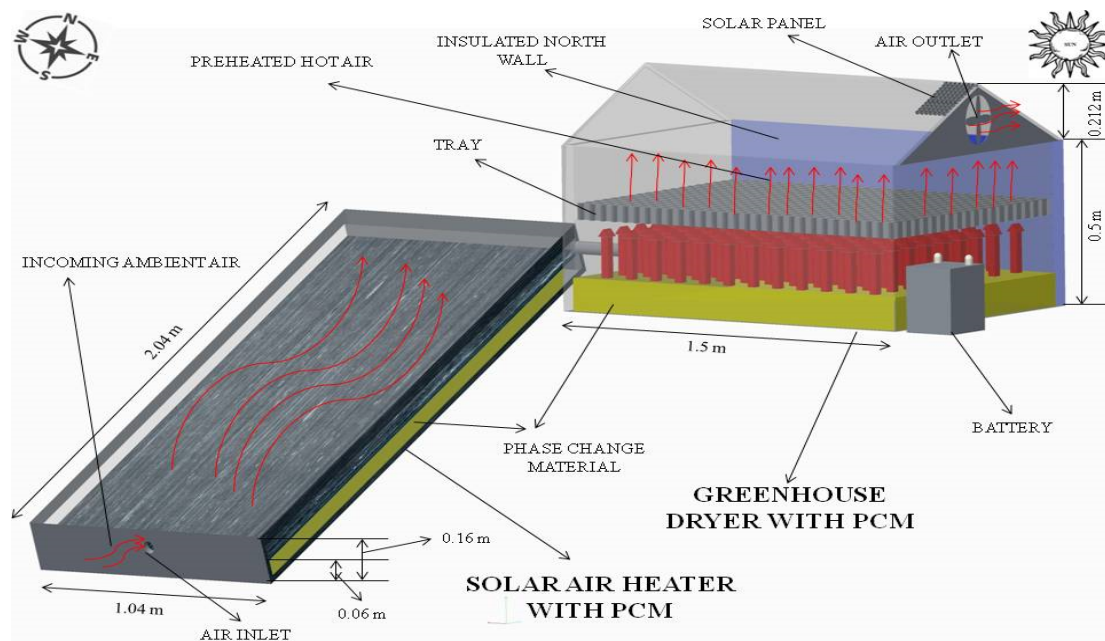


Figure 7. Hybrid greenhouse dryer.

4. Performance of Greenhouse Dryer in No Load Condition

The thermal performance indicator has been estimated for the heat storage-based greenhouse dryer operating in the passive, active, and hybrid modes.

4.1. Overall Heat Transfer Coefficient

The overall heat transfer coefficient (OHTC) measures the one dimensional steady-state heat transfer rate of the system [61]. It can be calculated using Equation (1):

$$\frac{1}{U} = \left(\frac{1}{h}\right) + \left(\frac{l_g}{K}\right) + \left(\frac{1}{h_{can}}\right) \quad (1)$$

Here, h is the heat transfer coefficient, l_g is thickness, K is thermal conductivity, h_{can} is the heat transfer coefficient for the canopy, and U represents the overall heat transfer coefficient. The relationship with U was also developed by Connellan, as per Equation (2):

$$U = 3.96 + 1.02V_{wd} \quad (2)$$

It has been further calculated as follows:

The quantitative characteristic of a convective heat transfer between the surface (wall) and a fluid (air) is termed as the heat transfer coefficient. It can be calculated as shown in Equation (3):

$$h = h_{gr} + h_{rm} + h_{evp} \quad (3)$$

where h_{gr} is the ground to room heat transfer coefficient and h_{rm} is the heat transfer coefficient at room temperature.

The available moisture content in the crop is determined by the evaporative loss. It can be evaluated as shown in Equation (4):

$$h_{evp} = 0.016h_{can} \left[\frac{P(T_{tr}) - \gamma P(T_{rm})}{T_{tr} - T_{rm}} \right] \quad (4)$$

where h_{evp} is neglected in accordance with the no-load condition [50].

The ground to room air heat transfer coefficient is evaluated as shown in Equation (5):

$$h_{gr} = 0.884 \left(T_{grd} - T_{rm} + \frac{[P(T_{grd}) - \gamma P(T_{rm})](T_{grd} + 273)}{268.9 \times 10^3 - P(T_{grd})} \right)^{\frac{1}{3}} \quad (5)$$

The greenhouse room air heat transfer coefficient is calculated as per Equation (6):

$$h_{rm} = \sigma \varepsilon \frac{\left[(T_{grd} + 273.15)^4 - (T_{rm} + 273.15)^4 \right]}{T_{grd} T_{rm}} \quad (6)$$

where, T_{grd} is the ground temperature, T_{rm} is the room temperature, σ is the Stefan Boltzman Constant, ε is emissivity, γ is relative humidity, and P is vapor pressure.

The thermal conductivity equation is shown in Equation (7):

$$K = 0.0244 + 0.7673 \times 10^{-4} T_{mean} \quad (7)$$

The canopy heat transfer coefficient is evaluated as shown in Equation (8):

$$h_{can} = 7.2 + 3.8V_{Wind} \quad (8)$$

Vapor pressure at temperature T is evaluated as shown in Equation (9):

$$P(T) = \exp \left(25.317 - \frac{5144.0}{T_{mean} + 273.15} \right) \quad (9)$$

The mean temperature can be calculated as shown in Equation (10):

$$T_{mean} = \frac{T_{tr} + T_{rm}}{2} \quad (10)$$

4.2. Dimensionless Number of the Experiments

To study heat transfer, dimensionless numbers are important tools. These tools are also used in the analysis of the convective heat transfer coefficient [49].

The Grashof number (Gr) is the ratio between the buoyancy force and viscous forces. The Gr number explains the effect of the hydrostatic lift force and the viscous force of air in the setup that is operating under passive mode conditions. It can be evaluated as per Equation (11).

$$Gr = \frac{X^3 g \beta \Delta T}{\nu^2} \quad (11)$$

where X is the characteristic dimension parameter, g is acceleration due to gravity, β is the coefficient of thermal expansion, ΔT is the difference between the surface and the fluid temperature, and ν is the kinematic viscosity of the fluid.

The Raleigh number (Ra) is the product of the Grasoff number and the Prandtl number. It can be evaluated as per Equation (12).

$$\text{Ra} = \text{Gr} \times \text{Pr} = \frac{X^3 g \rho^2 \beta C_p \Delta T}{k \mu} \quad (12)$$

where C_p is the specific heat, ρ is the density of the fluid, k is thermal diffusivity, and μ is the dynamic viscosity of fluid. The Nusselt number (Nu) is defined as the progress of the heat transfer at the canopy of the proposed experimental setup to the air boundary. Moreover, it is the ratio between convective heat transfer and heat transfer through conduction in a fluid. It can be evaluated as per Equation (13).

$$\text{Nu} = \frac{h_c X}{K} \quad (13)$$

where h_c is the heat transfer coefficient and K is thermal conductivity.

The ratio between the momentum diffusivity and the thermal diffusivity characterizes the relationship between heat transfer and the air motion; this is called the Prandtl number (Pr).

It can be evaluated as per Equation (14).

$$\text{Pr} = \frac{C_p \mu}{K} \quad (14)$$

where X can be evaluated as per Equation (15).

$$X = \frac{L + B}{2} \quad (15)$$

When using the active mode or forced convection mode, the dimensionless parameter (i.e., the Reynold number) is calculated, whereas the Nusselt number and Prandtl number can also be calculated in the same manner as the passive mode [49]. The Reynold number can be analyzed as per Equation (16).

$$\text{Re} = \frac{\rho V X}{\mu} \quad (16)$$

where V is the flow speed.

4.3. Coefficient of Diffusivity

The instantaneous thermal loss factor (η_{in}) provides the drying time and it enhances the rate of moisture removal [34].

Indirect loss and direct loss are the types of losses that are accounted for with the instantaneous thermal loss factor. Equation (17) describes indirect loss, and Equation (17) describes direct loss [62].

$$\eta_{in,c} = \frac{U \sum A_i (T_{gr} - T_{amb})}{I A_{tr}} \quad (17)$$

$$\eta_{in,v} = \frac{\left(c_d n A_v \sqrt{\frac{2 \Delta P}{\rho_r} \Delta P} \right)}{I A_{tr}} \quad (18)$$

$$\eta_{in,v} = 1 - \eta_{in,c} \quad (19)$$

The coefficient of diffusion is calculated using Equation (20):

$$C_d = \frac{(1 - \eta_{in,c}) I_{gh} A_{tr}}{(n A_v (\frac{2\Delta P}{\rho})^{\frac{1}{2}} \times \Delta P)} \quad (20)$$

where ΔP can be calculated by adapting Equation (21):

$$\Delta P = P(T_{rm}) - \gamma P(T_{amb}) \quad (21)$$

where A_{tr} is the area of the tray, I is the solar intensity, T_{gr} is the greenhouse room temperature, ρ_r is the density of room, ΔP is the partial pressure difference, A_v is the area of the vent, n is a component found in no-load conditions, c_d is the coefficient of diffusivity, $\eta_{in,v}$ is the instantaneous thermal loss at the vent, and $\eta_{in,c}$ is the instantaneous thermal loss that occurs at the canopy.

4.4. Heat Loss Factor

Due to the low density, the excess amount of air in the greenhouse dryer moves in the direction of the ventilator; this is called the heat loss factor [63]. This is evaluated in accordance with Equation (22):

$$Q_{loss} = C_d \times A_v \times \left(\frac{2\Delta P}{\rho}\right)^{\frac{1}{2}} \times \Delta P \quad (22)$$

The heat loss due to the exhaust fan in the forced convection mode of the heat storage-based greenhouse dryer can be calculated as per Equation (23)

$$Q_{loss} = 0.33 N V_g (T_{rm} - T_{amb}) \quad (23)$$

where N is the number of air exchanges per hour and V_{gi} is the volume inside of the greenhouse dryer.

4.5. Heat Utilization Factor

The heat utilization factor is the ratio between the difference between the ground temperature and the room temperature, and the difference between the ground temperature and the ambient temperature, during the drying process [64]. This parameter is calculated in accordance with Equation (24):

$$HUF = \frac{T_{grd} - T_{rm}}{T_{grd} - T_{amb}} \quad (24)$$

4.6. Air Exchange per Hour

Numerous air exchanges/h (N) happen by the exhaust fan in the proposed greenhouse dryer. These exchanges predominantly rely on the limitations of the exhaust fan, particularly its rpm and the number of fans utilized in the ventilator. It tends to be determined in accordance with Equation (25) [64].

$$N = \frac{V_{oc} \times A_{cv}}{V_{gi}} \times 3600 \quad (25)$$

4.7. Electrical Efficiency and Solar Photovoltaic System (SPV) Efficiency

The PV module efficiency is determined as per Equation (26)

$$\eta_{ee} = \left[\frac{0.8 \times I_{sh} \times V_{oc}}{I_{gsr} \times A_{sc}} \right] \times 100 \quad (26)$$

The solar photovoltaic system comprises a sunlight-based module, a battery, a sun-powered charge regulator, and a DC exhaust fan. The solar photovoltaic system's (SPV) effectiveness can be determined as per Equation (27).

$$\eta_{spv} = \left[\frac{V_{LV} \times I_{LC}}{I_{gsr} \times A_{sc}} \right] \quad (27)$$

where V_{oc} is the voltage of the open circuit, A_{cv} is the cross-section area of the ventilator, V_{gi} is the volume inside of the greenhouse dryer, I_{sh} is the short current, I_{gsr} is the global solar radiation, A_{sc} is the area of the solar cell, V_{LV} is the load voltage, and I_{LC} is the load current.

5. Performance of the Greenhouse Dryer under Load Conditions

The thermal performance indicator has been estimated for the heat storage-based greenhouse dryer operating in active, passive, and hybrid modes.

5.1. Ratio of Moisture (M_{ratio})

The moisture content (M_{ini}) for crops and the basis for wetness (w.b.) were calculated as per Equation (28):

$$M_{ini} = \frac{W_{ini} - W_{hr}}{W_{ini}} \times 100 \quad (28)$$

where W_{ini} is the initial weight of the crops, whereas W_{hr} is the weight of the crops on an hourly basis. The computation of the final and initial moisture contents help calculate the total removal of water content (W_{ttl}) from the crops [5]. It can be evaluated as per Equation (29):

$$W_{ttl} = \frac{M_{ini} - M_{fnl}}{100 - M_{fnl}} \times W_{ini} \quad (29)$$

where M_{ini} is the initial moisture content with regard to the basis of wetness, and M_{fnl} is the final moisture content with regard to the basis of wetness.

The instantaneous moisture content with regard to the basis of dryness can be calculated at a specific time (M_{ins}), as per Equation (30) [65]:

$$M_{ins} = \left[\frac{(M_{ini} + 1)W_{hr}}{W_{ini}} - 1 \right] \quad (30)$$

The moisture ratio (M_{ratio}) can be calculated as per Equation (31) [66]:

$$M_{ratio} = \frac{(M_{ins} - M_{eqm})}{(M_{ini} - M_{eqm})} \quad (31)$$

where M_{eqm} is the equilibrium moisture content and M_{ini} is very high compared with M_{eqm} ; thus, the abovementioned equation can be expressed in accordance with Equation (32):

$$M_{ratio} = \frac{M_{ins}}{M_{ini}} \quad (32)$$

The drying rate of the crop can be determined as per Equation (33):

$$DR = \frac{M_{evp}}{DM \times t} \quad (33)$$

where M_{evp} is the level of moisture evaporated per kg, DM is the amount of dried mass per kg, and t is the time required for drying.

5.2. Drying System Efficiency (η_{hgd})

Drying system efficiency was achieved with the help of an equation based on exhaust fan energy consumption. This is shown in Equation (34) [5]:

$$\eta_{hgd} = \frac{W_{ttl} \times h_{lh}}{A_{tr} \times I_{grd}} \quad (34)$$

6. Thermal Modelling of Greenhouse Dryers

6.1. Necessity of Thermal Models

This experiment is costly and time-consuming; thus, thermal modelling is the best option for enhancing the dryer's operational parameters. Software helps to make the analysis more exact, quicker, and simpler.

Thermal modelling is an economic model and it can be used for designing greenhouse dryers. It can also be used to achieve the maximum efficiency. During the design stage, thermal model simulation results are useful for investigating certain parameters. The greenhouse dryer performance depends upon the assessment of the heat transfer coefficients. The moisture content of agricultural produce is significant for the computation of the dryer's performance and the drying rate. The moisture content ratio is shown as a function of time from the experimental data, and the data is fitted with theoretical models that are available in the literature using statistical parameters. The constants and correlation coefficients in the empirical models have no physical significance. The moisture content plot determines data fitting and constant estimation. Additionally, the mean absolute error, the root mean square error, and the reduced chi-square are computed in order to identify the best-suited model. The thin layer drying models are developed from Newton's rule of cooling (Newton, Page, and Modified Page model), Fick's second law of diffusion (Henderson and Pabis model), and the others are empirical models (Thompson and Wang model; Singh model). Table 1 lists the equations for several frequently used thin-layer drying models.

Table 1. Thermal Models [67].

Sl. No.	Thermal Models	Equations
1	Newton	$M_{ratio} = \exp(-kt)$
2	Henderson and Pabis	$M_{ratio} = a \exp(-kt)$
3	Wang and Singh	$M_{ratio} = 1 + ax + bx^2$
4	Page	$M_{ratio} = \exp(-kt^n)$
5	Logarithmic	$M_{ratio} = a \exp(-kt) + c$
6	Prakash and Kumar	$M_{ratio} = at^3 + bt^2 + ct + d$
7	Ahmad and Prakash	$M_{ratio} = a \exp(-kt^n) + bt^2$

6.2. Thermal Modelling of Solar Greenhouse Drying Systems

Thermal modelling solar greenhouse drying systems is necessary to optimize the various heating designs and operation parameters. The fan system, earth-air heat exchanger, greenhouse room air temperature, ground air collector, greenhouse floor, canopy cover, insulation on north wall, the storage capacity inside the greenhouse dryer are the components of a greenhouse dryer [2,66].

6.2.1. Thermal Modelling of Natural Convection Solar Greenhouse Dryer

Tiwari et al. (2004) worked on the drying process of jaggery, and they evaluated the mathematical modelling used for calculating the convective mass transfer coefficient when roof-type natural convection solar greenhouse dryers are used. Jaggery temperatures, the mass evaporated, the relative humidity, and the greenhouse room air temperature was measured in order to calculate the mass transfer coefficient for convection. The convective

mass transfer coefficient was largest first, and it gradually decreased as drying continued. In this experiment, the convective mass transfer coefficient ranged between $1.28 \text{ W/m}^2 \text{ K}$ and $1.41 \text{ W/m}^2 \text{ K}$ [68].

Kumar and Tiwari (2006) created a thermal model for calculating the hourly estimates of the jaggery temperature, the greenhouse air temperature, and moisture evaporation in a span roof-type greenhouse drying system for drying jaggery under natural convection conditions. The experimental and anticipated values were determined to be effective. For greenhouse air and jaggery temperatures, the coefficient of correlation was 0.9–0.99, and the mass was 0.96–1. The mass of the jaggery and the thin layer that helped to establish the thermal model was suggested to construct the greenhouse dryer [69].

Jain and Tiwari (2004) developed a mathematical model to investigate the thermal behavior of peas and cabbage during the drying process, as well as to forecast the room temperature, moisture evaporation, and crop temperature. The greenhouse and ambient characteristics were calculated using MATLAB software and they were experimentally tested. Using experimental measurements, the anticipated values were found to be effective. For the crop and dryer air temperatures, the coefficient of correlation ranged between 0.79 and 0.99. The crop mass when drying had a coefficient of correlation between 0.98 and 0.99 [51].

Sacilik et al. (2006) analyzed mathematical modelling for sun tunnel drying systems for thin layers of tomato (organic). This technology lowered the initial expenditure during the dryer manufacturing while improving the product [70].

Janjai et al. (2011) used thermal models to forecast greenhouse dryer performance for dry chilis, bananas, and coffee. For the purpose of performance evaluation, many characteristics such as relative humidity, air temperature, and moisture content were taken into account. To develop the mathematical models, certain assumptions were made: the air flow in the dryer was unidirectional, there was no stratification, the drying calculation was based on the thin layer drying model, and the specific heat used for the cover, product, and air were all constant. It was discovered that there was a reasonable degree of consistency between the theoretical and experimental moisture contents of coffee, bananas, and chili during the drying process [71].

Turhan (2006) used thermal modelling to assess the heat uptake and thermal efficiency of natural convection greenhouse dryers under both no-load and load conditions. The dryer was also tested without a chimney and with a chimney to see how the chimney affected the air flow. Due to the increased air velocity, the dryer assisted by a chimney provided an enhanced mass flow rate [72].

These dryers were proven to be very useful in wet, high, and relatively humid climates.

6.2.2. Thermal Modeling of a Forced Convection Solar Greenhouse Dryer

Thermal modelling was used by Tiwari et al. (2004) to determine the convective mass transfer coefficient for drying jaggery in a greenhouse dryer under forced convection conditions. The room temperature, jaggery temperature, the mass evaporated, and the relative humidity were used to compute the convective mass transfer coefficient; this varied between 1.5 and $1.7 \text{ W/m}^2 \text{ K}$. This value is greater than the value obtained from the natural convection mode [71].

Kumar and Tiwari (2006) used thermal modelling to optimize the operating parameters of a greenhouse drying system for drying jaggery under forced convection conditions. The coefficient of correlation was found to be between 0.97 and 0.97, and the square root of the percentage variation was found to be between 6.78 and 12.72 percent, thus indicating that the predicted and experimental findings were in accordance with one another. The flow rate of air had a substantial impact on drying jaggery [69].

Condori and Saravia (1998) created a model to better recognize the evaporation rate in single and double chamber forced convection greenhouse drying systems. Regarding the modelling, the drying kinetics of the product, as well as the dryer design characteristics, was considered. The dryer performance curve and the generalized curve were also introduced.

The generalized drying curve serves as a reference for operational parameters, time variable factors, and solar energy, whereas the dryer performance curve depicts the production efficiency. Based on the simulation findings, it was determined that only a few system functions can improve the drying potential, in addition to the production rate, which would subsequently increase [58].

To estimate the performance of the tunnel-type greenhouse dryer, Condori and Saravia (2003) created an analytical model. The greenhouse was used as a solar collector in this investigation. The incidental solar radiation and greenhouse outlet temperature were found to have a linear relationship. Using the dryer's characteristic functions, the dryer's performance was assessed [73].

Jain (2005) suggested a transient analytical model. The packed bed thermal storage was installed against the dryer's north wall. The north wall achieved a temperature of 86 °C during peak solar radiation hours. Thermal energy storage has a considerable impact during cloudy hours, and it may be particularly effective in reducing temperature fluctuations during the drying process. The presented model is beneficial for predicting greenhouse dryer performance [74].

Prakash and Kumar (2013) conducted a full thermal analysis of the improved active greenhouse dryer in no-load mode. To prevent direct solar energy loss, a black PVC sheet was laid on the greenhouse floor, and a mirror was installed on the north wall. The dryer was placed on the barren concrete floor on the first day in order to grasp the effectiveness of the system, and it was placed on the black PVC sheet on the second day in order to understand the effectiveness of the system. The goal was to ascertain how successful the modified dryer was with regard to drying crops with a higher moisture content. All of the adjustments were determined to be appropriate for agricultural products with greater moisture contents [50].

Thermodynamic modelling and the experimental validation of a PV-ventilated solar greenhouse dryer for peeled longan, banana, tomatoes, and macadamia nuts, were presented [75]. To explain heat and mass transfer during drying, partial differential equations were created and solved numerically using the finite method. This model provides the best greenhouse dryer design data. To investigate the effectiveness of a battery-operated walk-in type of solar tunnel dryer for drying surgical cotton produced in Udaipur (India), Panwar et al. (2013) used thermal modelling. The dryer had a capacity of 600 kg, and it could reduce the moisture content from 40 to 5% in a single day [76].

Thermal modelling was used by Barnwal and Tiwari (2008) to investigate the convective heat transfer coefficient for drying of grapes in a PV/T hybrid greenhouse dryer [77].

7. Environomical Analyses of Greenhouse Dryer

Due to the rise in fuel costs, the cost of the materials, and the higher energy impact of the energy system, the need for energy analysis becomes very important for any energy system; therefore, for the proposed drying system, it was important to conduct an environomical analysis [78].

7.1. Embodied Energy

Embodied energy is defined as the total energy required for producing any product or service [79].

7.2. Energy Payback Time (EPBT)

The energy payback period is the required time to recover the embodied energy of the product. It is determined in accordance with Equation (35) [80]:

$$EPBT = \frac{E_{emd}}{AE_{output}} \quad (35)$$

where E_{emd} is embodied energy and AE_{output} is the annual energy output.

Therefore, the energy payback time relies on embodied energy and the annual energy output.

7.3. CO₂ Emission

The average CO₂ emissions for electricity generated by coal, as suggested by Prakash and Kumar, are approximately equivalent to 0.98 kg of CO₂/kWh [81]. The lifetime of the north wall that insulated the greenhouse dryer was found to be 35 years [82]. The CO₂ emissions per year can thus be calculated as per Equation (36):

$$\text{CO}_2 \text{ Emission per year} = \frac{E_{emd} \times 0.98}{L} \quad (36)$$

where L is the lifetime of the proposed system.

7.4. Cost Analysis

The payback period of the dryer is calculated as:

$$N = \frac{\ln(1 - \frac{D_c}{s}(d_i - f))}{\ln\left(\frac{1+f}{1+d_i}\right)} \quad (37)$$

where D_c is the dryer cost, d_i is the rate of interest, and f is the rate of inflation.

7.5. Carbon Mitigation and Earned Carbon Credit

To measure climate change potential, measures to mitigate carbon dioxide emissions should be undertaken. This can conveniently be compared with other power production systems because the unit of measurement for the mitigation of net CO₂ emissions is per kilowatt hour. Defining carbon credit is a key component of national and international emission trading schemes that have been implemented in order to mitigate global warming. Minimizing the effects of greenhouse emissions on a commercial scale occurs when the total annual emissions are capped; this provides an opportunity to compensate for any shortfall that may occur when the assigned mitigation level is not reached. Given the current prices, the exchange of carbon credit can be bought and sold in international markets or between businesses. Carbon credit may be utilized in financial carbon reduction schemes [83]. The daily thermal output, daily thermal input, and annual thermal output energy can be calculated using Equations (38)–(40):

$$E_{an} = \text{Daily thermal output energy of dryer}(E_d) \times N_d \quad (38)$$

$$E_d = \frac{M_{evt} \times L_{ent}}{3.6 \times 10^6} \quad (39)$$

$$\text{Daily input energy} = I_g \times N_h \times A_c \times 10^{-3} \text{ kWh} \quad (40)$$

where M_{evt} is the moisture evaporated, L_{ent} is the latent heat of evaporation, N_d is the total number of sunny days in a year (i.e., 300 days), E_{an} is the annual thermal output energy, A_c is the area of the solar collector, and N_h is the number of sunny hours per day.

Coal-based power was calculated to be 0.98 kg of CO₂/kWh as a result of the mean CO₂ equivalent intensity; therefore, the amount of CO₂ that is mitigated by the system would be calculated as per Equations (41) and (42).

$$\text{Lifetime mitigation of CO}_2(\text{kg}) = \text{Total CO}_2 \text{ mitigation} - \text{Total CO}_2 \text{ emission} \quad (41)$$

$$\text{Lifetime mitigation of CO}_2(\text{kg}) = [(E_{an} \times n) - E_m] \times 2.01 \quad (42)$$

where Em is embodied energy in kWh and n denotes the lifespan of the dryer, which is 35 years. The earned carbon credit was calculated as per Equation (43)

$$\text{Earned carbon credit} = \text{net mitigation of CO}_2 \text{ in lifetime (tone)} \times D \quad (43)$$

Here, the cost of carbon credit is denoted by D which varies between USD5–20/ton of CO_2 that is mitigated.

8. Analysis on the Recent Trends of Greenhouse Dryers

The proper drying techniques are profitable for reducing the post-harvest losses of agricultural products [84]. The use of solar energy has been used for drying purposes since ancient times. GHD is one of the techniques used for the preservation of agricultural products that will be consumed in the future [85]. Experiments conducted by earlier investigators demonstrate that drying is an energy-intensive operation. The complex processes comprising heat and mass transfer are involved in drying the drying medium and the product [86]. In order to meet the increasing demand for food preservation, research has continuously been conducted on greenhouse drying methods in order to develop cheap, simple, and efficient solar dryers which are independent of seasonal vagaries [87]. Many studies, from all over the world, have consistently focused on drying applications and the design of solar dryers.

The recent developments in greenhouse dryers are predominantly based on reducing the length of the drying period, improving the efficiency of the dryer, and productively utilizing solar energy. There have been many innovative techniques applied to greenhouse dryers, such as the use of Phase Change Materials (PCMs), integration with solar air dryers, closed loop operations (automated), and so on. In this paper, greenhouse dryer development analysis is evaluated based on the dryers' performances, the impact on the environment, and economic parameters.

The drying rate, specific moisture extraction, thermal and overall efficiency, coefficient of performance (COP), rate of energy extraction, payback period, and so on, are the main parameters that help to determine the greenhouse dryer performance analysis. Performance analysis parameters help to evaluate how new modifications installed on the dryer work.

8.1. Studies Conducted on Natural Convection Greenhouse Dryers

The batch type industrial dryer was developed by Mathionlakis et al. (1998) for drying vegetables and fruits. CFD FLUENT software helps to replicate the air movement within the drying room. The considered boundary conditions include the fixed mass inflow boundary condition, the no resistance boundary condition and the wall shear stress condition on the bounding domain. Differences between the dryers in several trays were noticed. In some regions of the chamber, non-uniformity was traced. The recorded data available from drying tests and the CFD illustrated a good correlation between the drying rate and the air velocity [88].

Bartzanas et al. (2004) has used FLUENT v.5.3.18 software to conduct the CFD simulation. The simulation was conducted in order to recognize the effects of the vent arrangement on air ventilation inside the tunnel type greenhouse dryer. A commercial CFD code was used for several investigations, such as the impact of configuring a tunnel greenhouse dryer, the ventilation, temperature, and crop airflow patterns. Validating the mathematical model against empirical data was also ascertained. A three-dimensional sonic anemometer was used to determine the airflow patterns, and a tracer gas technique was applied to drive the greenhouse ventilation rate. To study the outcome of four different configurations of the natural ventilation system, the CFD model was used. The ventilation configuration influences the air temperature distributions and the ventilation rate of the greenhouse dryer. It was noted that the computed ventilation rates and the different configurations varied between 10 and 58 air changes/h for an outside wind, with a wind speed of 3 m/s. The wind direction is perpendicular to the openings. The mean air temperature in the middle of

the solar tunnel varied from 28.2–29.88 °C when the outside air temperature was recorded at 28 °C [89].

A mathematical model was developed by Jain and Tiwari (2004b) to study the thermal behavior for drying peas and cabbage. Predictions for the greenhouse room air temperature, the crop temperature, and the moisture evaporation rate were made. For computation, MATLAB software was conveniently used for the different greenhouse and ambient parameters. The model was empirically validated. There was a satisfactory agreement between the predicted values and experimental findings. The coefficient of correlation between the crop and the greenhouse room air temperature ranged between 0.77 and 0.97. During drying, the coefficient of correlation for the crop mass ranged between 0.98 and 0.99 [51].

Tiwari et al. (2004) evaluated the convective mass transfer coefficient for drying jaggery inside a roof-type even span greenhouse dryer operating under natural convection conditions. During the experiment, a variety of parameters were measured, such as relative humidity, greenhouse room air temperature, mass evaporated during the drying process, and the temperature of the jaggery. The data collected was utilized in order to evaluate the convective mass transfer coefficient favorably. There was an initial increase in the convective mass transfer coefficient rate, which gradually decreased as the drying process continued. It was experimentally established that the convective mass transfer coefficient varied from 1.29–1.41 W/m²·K under natural convection drying conditions [68].

Sacilik et al. (2006) presented a mathematical model demonstrating the effects of the solar tunnel drying system that was exposed to ecological conditions in Ankara, Turkey, when drying a thin layer of a tomato. The organic tomatoes were dried using open sun drying and with a solar tunnel drying system. The duration of time required for the drying process to obtain a predetermined final moisture content of 11.5% from an initial moisture content of 93.35% (w.b.) using a solar tunnel drying system and open sun drying was four days and five days, respectively. Mathematically calculating the diffusion model reduces the root mean square error because of the higher coefficient of determination; thus, it is opined that this model will reduce the monetary value of drying by obtaining a better quality of dried products [70].

Kumar and Tiwari (2006) developed a thermal model that was capable of predicting and recording the greenhouse air temperature, moisture evaporation rate, and jaggery temperature hourly when using the greenhouse drying system for the complete drying process of jaggery under natural convection conditions. The investigated analysis and the predicted values were in close agreement. The coefficient of correlation for greenhouse air and the jaggery temperature ranged between 0.90 and 0.98 and the jaggery mass during drying ranged between 0.96 and 1.00. The thermal model was proposed as being very conducive when designing the greenhouse dryer, and for investigating a thin layer of the known mass of jaggery [54].

Turhan (2006) proposed two new heavy-duty greenhouse dryers that operated under natural convection conditions. These dryers were examined under both load and no-load conditions. The comparative analyses were conducted after drying the same amount of pepper in a dryer and under the same climatic conditions. The pepper placed in the dryer was found to be of superior quality after drying. In comparison with open sun drying, the proposed dryer was found to be two and a half times (250%) more efficient [72].

The effects of airflow have also been analyzed by examining the dryers with and without a chimney. The results of the experiments revealed that the greenhouse dryers increase the inside air temperature by 5 to 9 °C compared with the ambient temperature. The chimney of the dryer facilitates a better airflow by enhancing the air velocity. It was also concluded that to avoid spoilage and to maintain the nutritional value of the product; these dryers must be successfully employed to dry various agricultural products such as fruits and vegetables. These dryers, in particular, are better utilized in wet areas or in climatic zones with high density [87].

Janjai et al. (2011) predicted the performance of a greenhouse dryer that dried bananas, chilis, and coffee by developing a thermal model. Parameters such as temperature,

relative humidity, and moisture content were analysed. A comparative analysis of a solar greenhouse dryer was conducted under open sun drying conditions. The same quantity of bananas was taken and exposed for an equal time of five days. The moisture content differed between 68 and 20% (w.b.) in the greenhouse dryer, whereas it differed between 68 and 29% (w.b.) under natural sun drying conditions.

Similarly, the moisture loss regarding chilis was reduced from 75 to 15% (w.b.) in the greenhouse dryer within three days. In contrast, using an identical quantity and time duration, the moisture content of the chilis when exposed to open sun drying conditions was only reduced from 75 to 42%.

The moisture content with respect to coffee was reduced from 52 to 13% (w.b.) within two days, whereas under natural solar drying conditions, to reach the final moisture content value, it took four days; thus a realistic agreement was found between the theoretical and experimental moisture contents of chilis, bananas, and coffee [71].

Prakash and Kumar (2014) presented the ANFIS (Adaptive Neuro-Fuzzy Inference System) model for the drying of jaggery in the greenhouse dryer under natural convective conditions. The aim of the experiment was to forecast the jaggery temperature, the greenhouse air temperature, and the moisture evaporation for the jaggery, which was placed inside the greenhouse dryer, which operated under natural convection conditions. For drying jaggery, a roof-type even spans greenhouse dryer was selected, with a floor area of $1.20 \times 0.78 \text{ m}^2$. MATLAB software develops the ANFIS model, which was used to forecast the thermal performance of the greenhouse dryer based on the solar intensity and the ambient temperature. The developed model was experimentally validated, and it was found that there was good agreement between the experimental and analytical results for the drying of jaggery [90].

Prakash and Kumar (2016) recorded the thermal performance for a modified greenhouse dryer, subjecting it to natural convection and no-load conditions from January 2013 to May 2013. The concept of the opaque north wall was applied with three different floor conditions consisting of a barren floor, a black painted floor, and a black PVC sheet covered floor. The experiment was conducted in order to record the thermal performance of the dryer. Based on empirical data, different thermal performances, such as dimensionless numbers (Nusselt, Grashof, Prandtl, and Rayleigh numbers), the coefficient of diffusion, the heat transfer coefficient, and heat loss, were analyzed. The floor covered with a black PVC sheet was found to be the most useful for crop drying in the experimental study conducted by Prakash and Kumar. It provides a relatively higher room air temperature and lower room humidity [81].

Amjad et al. (2015) experimented on the flow simulation to predict the air distribution in the drying chamber (batch type dryer) for drying potato slices with a thickness of 4 mm using ANSYS-FLUENT CFD. A proposal including a diagonal airflow inlet channel that aligns with the length of the drying chamber was put forward for this dryer. The coefficient of correlation was recorded to be 87.09% for the airflow distribution of this experiment [91].

Chauhan and Kumar (2016) analyzed the performance of a greenhouse dryer with an insulated north wall under natural convection conditions in June 2011. Two separate experiments were conducted, one with a solar collector and another without a solar collector. A thermal analysis that took the coefficient of diffusivity, coefficient of performance, heat utilization factor, and convective heat transfer coefficient into consideration was evaluated. The difference between the highest convective heat transfer coefficients of the two cases was $29.09 \text{ W/m}^2\text{C}$. The inside room air temperature of the dryer for days 1, 2, and 3 were recorded as 4.11 %, 5.08%, and 11.61%, respectively. The inside room temperature of a dryer with a solar collector is comparatively higher than a dryer without a solar collector [64].

Chauhan and Kumar (2017) analyzed the performance of greenhouse dryer with an insulated north wall under natural convection and no-load conditions during October 2014. For two different cases (i.e., case I and case II), specific experiments were conducted. Case I described a greenhouse dryer with an insulated north wall that was assisted by a solar air heating collector on the ground's surface. In contrast, Case II described a greenhouse dryer

with an insulated north wall, without solar air heating collector, on the ground's surface. A performance analysis of the newly developed system based on the convective heat transfer coefficient, heat loss factor, coefficient of diffusivity, heat utilization factor, and coefficient of performance was conducted. The maximum relative value of the coefficient of performance and the heat utilization factor was recorded as being 0.9 and 0.68 for case I, and 0.86 and 0.61 for case II. For three days (i.e., Day 1, Day 2, and Day 3), the inside room temperature was recorded as being higher in comparison to ambient air at rates of 46%, 42%, and 32%, respectively. The developed system was thus recommended for fruit/vegetable drying based on results which validated the modification [49].

8.2. Studies Conducted on Forced Convection Greenhouse Dryers

Condori and Saravia (1998) modified a simple model to study the evaporation rate of two different types of forced convection greenhouse drying systems (i.e., one with a double chamber and the other with single chamber). The mathematical modelling for two kinds of dryers was taken into account for the dryer design parameters and the product drying kinetics. The two concepts introduced in this article were the dryer performance curve and the generalized drying curve. The generalized drying curve served as a reference for the time-variable parameter, as well as for the received energy from the sun parameter, and the operative parameters. The dryer performance curve delineated production efficiency. The drying potentials, product water content, and metrological variables were calculated using two non-dimensional variables. After the simulation and calculations, the author decided that incorporating some developments into the system could favorably improve the drying potential, which, in turn, could further enhance the production rate. With identical drying areas, regarding the double chamber system, the productivity increased by 87%, compared with the single-chambered system. To further reduce the drying cost, some essential changes were made to the double chamber drying system in order to make it more simple and less expensive [58].

An analytical model was developed by Condori and Saravia (2003) to study the performance of the tunnel type greenhouse dryer. The greenhouse was assumed to be a solar collector. A linear function was obtained between the incidental solar radiation and the greenhouse output temperature. The dryer's characteristic functions determined dryer performance. It was observed that almost constant production occurred daily. As compared with the single-chamber dryer, an improvement of 160% in production was seen in the simulation test on red sweet pepper, whereas in the case of the double chamber dryer, the improvement was only 40% [73].

Tiwari et al. (2004) measured the convective mass transfer coefficient for drying jaggery under forced convection conditions in the roof type even span greenhouse dryer. Dissimilar parameters were calculated at the time of the experiment, such as greenhouse room air temperature, the temperature of jaggery, relative humidity, and mass evaporated. The range of the convective mass transfer was found to be between $1.3 \text{ W/m}^2\cdot\text{K}$ and $1.46 \text{ W/m}^2\cdot\text{K}$. The data certified that the convective mass transfer coefficient for the forced convection mode was higher than the natural convection mode [68].

Jain and Tiwari (2004) examined thermal modelling in order to study behavioral patterns when drying cabbage and peas that were subjected to forced convection conditions; these conditions were based on ambient temperature and solar intensity for the prediction of the rate of evaporation, crop temperature, and greenhouse air temperature. The experimental value and predicted values were found to be in good agreement in terms of percentage deviation and root square error. The range for the coefficient of correlation and root mean square error was recorded as 0.92–0.99 and 3.88 to 8.43, respectively [92].

Jain (2005) proposed a transient analytical model to study the effect of the packed bed thermal storage inside the even span greenhouse dryer. The packed bed thermal storage was used to replace the north wall of the dryer. The performance evaluation of a crop was undertaken by using onion for the case study. The dimensions of the greenhouse drying system were 6 m in length, 4 m in breadth, and 0.25 m in height. For similar climatic

conditions, all the experiments were performed in May, in New Delhi, India. The focus of this experiment was to study the effect of the mass flow rate of air, the dimensions of the greenhouse dryer, and the temperature of the crop. Initially, it was found that the rate at which the removal of moisture occurred, in addition to the drying rate, was rather high, but after 4 h, the rate at which the removal of moisture occurred, and the drying rate of the crop diminished considerably. The temperature of the north wall of the dryer reached 84 °C when operating during peak solar radiation hours. During the 24 h study it was observed that when 2280 kg of onion was allowed to lose moisture and be dried at an effective height of 0.25 m, the mass flow rate was recorded as being 0.278 kg/s. The initial moisture content was recorded as 6.14, and it was reduced by up to 0.21 kg water/kg of dry matter. The thermal energy storage had a significant effect, even in off-peak sunshine hours, and it proved to be useful for the reduction in temperature fluctuations. The proposed model was found to be very useful in the performance analysis conducted by the author [74].

Kumar and Tiwari (2006) performed thermal modelling of a greenhouse drying system for drying jaggery under forced convection conditions. In this experiment, the roof type even spans greenhouse dryer, with a $1.20 \times 0.78 \text{ m}^2$ floor area, was used to dry 2 kg of jaggery that was specifically prepared with dimensions of $0.03 \times 0.03 \times 0.03 \text{ m}^3$. For four consecutive days in March, the experiments were performed in the IIT Delhi, and data were recorded on an hourly basis. The effects arising from changes in the air, relative humidity, air temperature, and changes in the mass of the jaggery was observed on an hourly basis. The experimental and theoretical results show a perfect agreement that is reflected through the records wherein the coefficient of correlation ranges between 0.96 and 0.98. Moreover, the percentage of the square root of deviation ranged between 6.75 and 12.63%. During experimentation, it was observed that the number of air changes per hour had a remarkable effect on greenhouse air temperature and drying jaggery. With the increase in the number of air changes per hour, there was a decrease in greenhouse air temperature [69].

Janjai et al. (2009) developed the PV- ventilated solar greenhouse dryer to conduct a performance analysis of the process wherein peeled longan and bananas are dried. A parabolic roof, covered with polycarbonate plates that have a concrete floor, constituted the structure of the dryer. A 50 W photovoltaic module runs three fans to ventilate the air from the dryer. To study the performance of the greenhouse dryer, five experiments were conducted separately to dry both bananas and peeled longan. The temperature range varied when drying peeled longan, from 30 to 58 °C, and when drying bananas, the temperature varied between 30 and 60 °C. The drying time for drying peeled longan and bananas using open sun drying was six days and five days, respectively. Moreover, under similar ambient conditions in a greenhouse dryer, it takes three days and four days, respectively. The experimental data obtained were used to develop a partial differential equation in order to describe the moisture and heat transfer at the time of drying the banana and peeled longan. It was further solved numerically using a finite difference method. These models may be utilized for providing optimal design data for greenhouse dryers [75].

Krawczyk and Badyda (2011) have developed a mathematical model for sewage drying that involves applying fluent computational fluid dynamics software in a forced convection GHD. The unsteady condition of the sludge inside the solar dryer was created in order to help the flow and thermal processes depending upon its thermodynamic characteristics and drying conditions (solar radiation, change over time, the humidity of ventilated air and temperature) [93].

Janjai (2012) developed a thermal model wherein a forced convection greenhouse dryer has a parabolic roof structure to dry tomatoes. Thermal modelling was conducted in order to investigate the performance of the dryer. The drying capacity of the greenhouse dryer was approximately 1000 kg. Hot air was supplied to the dryer continuously during the rainy season by attaching a 100 kW LPG gas burner onto the dryer. The dryer had to be utilized in order to dry the three batches of osmotically dehydrated tomatoes. When compared with open sun drying, this experiment illustrated that the drying time was reduced by 2–3 days and the drying air temperature of the dryer ranged between 35 and 65 °C [94].

Prakash and Kumar (2013) presented ANFIS (an adaptive neuro-fuzzy inference system) model to predict the relative humidity and the greenhouse air temperature in the modified greenhouse dryer operating under forced convection conditions. The experimental results validated the predicted values. A reliable correlation between the predicted and experimental data was found. The total magnitude of error was only 0.026 for the prediction of the greenhouse dryer's room air temperature [95].

A thermal model was developed by Tanwanichkul et al. (2013) to predict the convective mass transfer coefficient and to illustrate the strength of the sandwich type greenhouse dryer operating under forced convection conditions. The thermal behavior was analyzed during the process of drying a rubber sheet. A thermal model was applied to predict the temperature of each part of the greenhouse, including the drying chamber and rubber sheets. Some measures were necessary to simplify the model; however, a polycarbonate covering material and the heat capacity of the closed-in air were neglected. The premises were constructed so that there was no heat loss in terms of radiation, and the air medium within the social system did not participate in radiant energy transmission, and the shrinkage of the rubber sheet was negligible. The researchers further agreed that the absence of any heat conduction between walls was due to relatively small connecting areas and a low difference in temperature between the walls. In its quasi-steady-state, one-dimensional heat convection from the floor/wall to air was also conceived. The experimental determinations of these models were validated [96].

Prakash and Kumar (2014) have conducted the environmental analysis and prepared a mathematical model for drying tomato flakes in the modified greenhouse dryer operating under forced convection conditions. The moisture content of tomato flakes was initially noted as being 96.0% (wet basis), and it was reduced to 9.09% (wet basis) after 15 h of drying inside the dryer. In the environmental analysis, numerous economic and ecological parameters were evaluated, namely, the payback period, CO₂ emissions, energy payback time (EPBT), embodied energy, and the earned carbon credit. The coefficient of determination for the proposed drying model was recorded as 0.9985, and the embodied energy was recorded as 628.7287 KWh. The payback period, calculated according to the cost and energy payback time, was found to be 1.9 years and 1.14 years, respectively. The calculated CO₂ emission rate was estimated to be 17.6 kg/yr during its lifespan, and the calculated earned carbon credit ranged from 12,561.70 INR to 50,245.49 INR. The dried tomato flakes that were kept within the dryer were found to be of a better quality compared with those left in the open sun for drying [16].

Prakash and Kumar (2014) experimented upon, and conducted thermal analysis for, the modified solar greenhouse dryer operating under forced convection conditions for two consecutive days under no-load conditions. The dryer in this experiment was tested using a controlled air exchange rate. The intent was to identify the effectiveness of the dryer and to make it more efficient for drying products with higher moisture contents. A black PVC sheet was spread on the floor of the greenhouse dryer, and to reduce the direct loss of solar radiation, the north wall was fitted with a mirror. Two case studies were conducted in order to understand the efficiency of the system. In case I, the dryer was placed on the barren concrete floor, whereas in case II, the dryer was placed over a black PVC sheet. The atmospheric conditions of the sky were clear, and the wind speed was recorded to be low at 0–0.2 m/s. On day I, the maximum global radiation was 1061 W/m², whereas on day 2, it was recorded as being 978 W/m². The average ambient temperature on both days was 28.2 °C and 27.6 °C, respectively. The inside temperature was always higher in case II than case I, by 0 to 0.5 °C, as there was a reduction in heat loss because of the black PVC sheet. The relative humidity was identical on both days. The average equivalent thermal efficiency on day I and day II was recorded as 21.22% and 26.05%, respectively. The load efficiency and average convective heat transfer coefficient on day I and day II were recorded as (10.01% and 12.37%) and (7.41 W/m²°C and 16.6 W/m²°C), respectively [97].

Phusampao et al. (2014) installed an experimental greenhouse solar dryer in Loei Province, Thailand. The thermal modelling and testing of the dryer were conducted to

analyze the performance of the dryer when drying macadamia nuts. Six sets of macadamia nuts were put inside the dryer. Each batch of in-shell macadamia nuts was 730 kg. The drying time for the macadamia nuts was five days, as there had been a variation of 30 to 65 °C in the drying air temperature [98].

An indirect solar dryer was designed and constructed by Romero et al. for drying vanilla; it had a capacity of 50 kg. For simulation and validation, they opted for FLUENT ANSYS software. CFD was selected for temperature distribution analysis of the solar dryer. The temperatures at the outlet and inlet of the cabinet, and at the inlet of the solar collector, were taken. Three-dimensional temporary and laminar flows, for the CFD simulation, were considered. The three necessary parameters, which were the speed of the working fluid, the pressure, and the temperature, were recorded in order to explain the governing equations. Using the ANSYS FLUENT code, the physical phenomena were solved by applying four steps:

Step 1-The ANSYS design modeler program was used to design the geometry and discretization of the control volume.

Step 2-The specifications of the material properties and of each system's element boundary condition were given.

Step 3-To provide for each specified time interval, a solution of equations in every element of the mesh is provided.

Step 4-A graphical illustration of the results is obtained.

The application of measured parameters and the CFD simulation of the solar collector provided a superior degree of harmony. In contrast, in the case of a cabinet, a slide difference was noted between the estimated and measured temperatures. The variation was due to the convection heat transfer coefficient (constant) in the ambient case. It was illustrated that it was essential to define a convection heat transfer coefficient (variable) in terms of its ability to act as a function of time throughout the day, in order to predict the thermal parameter. Eventually, the weight loss of vanilla in one month time was recorded as being 62% (the initial weight being 1267.5 gm and the final reduced weight being 491.5 gm, respectively) for cabinet drying. In contrast, in the case of conventional drying, the same result takes three months [99].

Vintila et al. (2014) created a numerical simulation of an indirect solar dryer using COMSOL Multiphysics CFD. The numerical simulation was created using a reduced 2D domain model that used a COMSOL Multiphysics CFD commercial code, neglecting the effects caused by the side walls. The two elements are responsible for the physics settings of COMSOL (i.e., boundary conditions and subdomain settings). For the boundary conditions, boundary geometries are considered. Regarding the subdomain settings, modes of heat transfer (convection and/or conduction), types of material, and the initial conditions are taken into consideration. The simulation was executed on a sunny day when the sky was clear and solar irradiation was assumed to be 300 W/m². The backside of the collector and the walls of the drying cabinet were supposed to be adiabatic (thermally insulated). Different results were found after the completion of the analysis of the coupled thermal-fluid model pertaining to temperature distribution, velocity field, and pressure distribution in the solar collector. The drying chamber with different opening conditions, such as fully open, half-open, and fully closed conditions, was experimented upon to ascertain its various operational requirements. The predicted results were found to be very satisfactory when compared with the actual measurements [100].

Sethi and Arora (2009) worked on a conventional greenhouse dryer by using a reflecting aluminum sheet that was inclined at the optimum angle. The experiment was performed by using INWR for drying bitter gourd slices under both natural convection and forced convection conditions. The study found that the drying time for the product was reduced by using INWR. Compared with the natural convection mode, the forced convection mode of operation was found to be more effective [101].

Panwar et al. (2016) conducted thermal modelling upon the solar tunnel dryers operating with dry surgical cotton. The dryer capacity was 600 kg per day, and it was efficient

enough to reduce moisture from 40 to 5%. It was found that the drying air temperature was 2–3 °C more than the experimental values that were previously obtained [76].

Morad et al. (2017) designed three identical solar tunnel greenhouse dryers that operated under forced convection conditions. Thermal analysis was conducted for these dryers by using a thermal balance equation. The data obtained clearly illustrated that dried peppermint leaves were responsible for reducing the drying time and acquiring the highest percentage of volatile oil as compared with drying the whole of the plant. The peppermint was loaded onto a surface area of 4 kg/m² in the greenhouse dryer. The greenhouse dryer was operating under forced convection conditions. Peppermint was dried at a flow rate of 2.10 m³/min and the resultant rate of drying increased by 22.78% (for leaves) and 24.8% (for whole plants) [102].

Baniasadi et al. (2017) constructed a forced Convection mixed-mode solar dryer. It was used to dry fresh apricot slices. It consisted of a thermal storage unit that contained paraffin wax. It also contained a solar air collector, a photovoltaic panel, battery storage, and a single chamber in the drying system. The thermal performance of the system was studied by carrying out the experiments. It was found out that a 50% decrease in drying time occurred as a result of using thermal energy storage units [103].

Rabha et al. (2017) conducted experiments in order to ascertain the performance of a forced convection solar dryer, both in the presence and absence of paraffin wax. The time taken to achieve the final moisture content, using PCM, was four consecutive days, which was much lower than when PCM was not used [56]. The comparison of various types of greenhouse dryer has been illustrated in Table 2.

Table 2. Comparison of various types of greenhouse dryer.

Authors (Year) [Ref.]	Year	Types of Solar Dryer	Results/Significant Findings
Barnwal and Tiwari [77]	2008	Hybrid Photovoltaic-Thermal (PV/T) Greenhouse Dryer	Numerous experimental data, taken each hour, including grape surface temperatures, moisture evaporated, ambient humidity and air temperature, greenhouse humidity, and air temperature, were logged in order to assess the heat and mass transfer for the suggested system.
Tiwari et al. [104]	2016	Photovoltaic–Thermal (PV/T) Mixed Mode Greenhouse Solar Dryer	Thermal modelling for the PVT greenhouse dryer was created by taking into account several parameters such as crop, greenhouse, and solar cell temperatures, among others. Exergy and thermal energy have been determined.
Moreno et al. [105]	2016	Solar Greenhouse Dryer	Experimental drying of pinus pinaster wood chips occurred in a solar greenhouse dryer. The benefits of the solar greenhouse dryer, for both cases, included reaching 10% of relative humidity, and fewer days were required for this; such benefits were shown in the findings through mathematical modelling.
Morad et al. [102]	2017	Solar Tunnel Greenhouse Dryer	Three similar solar tunnel greenhouse dryers under forced conditions were erected to dry peppermint plants. In comparison with drying full plants, the data showed that drying peppermint leaves shortens the drying process and yields the largest percentage of volatile oil.
Chauhan and Kumar [49]	2016	Passive Greenhouse Dryer	The convective heat transfer coefficient, diffusivity coefficient, heat utilization factor, heat loss factor, and performance coefficient were evaluated as performance indicators for a newly constructed system.

Table 2. Cont.

Authors (Year) [Ref.]	Year	Types of Solar Dryer	Results/Significant Findings
Tham et al. [106]	2017	Solar Greenhouse Dryer Integrated with Heat Pump	An even span solar greenhouse dryer was created and used to dry Java tea and Sabah snake grass. Solar greenhouse dryers perform satisfactorily in clear weather, but they do not work as well at night or on wet days because of product rehydration, which is greatly influenced by high relative humidity in the surrounding air.
Janjai et al. [107]	2018	Parabolic Greenhouse Dryer	The performance of the dryer for drying litchi flesh was modeled using an ANN technique. The back-propagation approach was used to train the ANN model using drying data. Three sets of data were utilized to evaluate the ANN model, and seven different sets of data were used for training.
Khanlari et al. [86]	2019	Greenhouse Dryer	The drying time was significantly shortened by merging a T-SAH with a greenhouse dryer (GD). Additionally, the T-average SAH efficiency was found to be between 45.6 and 56.8%.
Aymen et al. [83]	2019	Solar Greenhouse Dryer	The findings of the experiment demonstrate that the experimental drying curves for drying red pepper lack a consistent rate period. Only the falling rate period is seen in the experimental drying curves. As a result, drying took two days instead of three in the SGD, and instead of three days in the open sun.
Huddar and Kamoji [108]	2019	Passive Solar Greenhouse Dryer	According to the trial findings, the drying chamber effectiveness was 51.7% and its typical drying speed was 0.158 kg/h. Moreover, 12.42 kWh/kg of a specific energy was consumed, and 1.27 kg (5.26%) of moisture content was removed. There was a 41.2% overall reduction in moisture content.

Regarding on Table 2, it is evident that the greenhouse dryer investigation shows that the greenhouse dryer is a very environmental methodology that minimizes the post-harvest losses of precious agricultural produce. Greenhouse dryers are mainly operated by two different modes of heat transfer, namely, passive and active modes. Greenhouse dryers are used for bulk-level drying. They are very effective for low-temperature thermal drying (<80 °C). In order to enhance their efficiency, various attempts have been made by various researchers; however, there is still scope for improvement.

8.3. Studies Conducted on Hybrid Greenhouse Dryers

Ferreira et al. (2007) introduced a hybrid solar electrical dryer consisting of a drying chamber and a solar chamber that was assisted by an electric air heater. The solar chamber was inclined at a horizontal angle of 30° and covered with glass. It opened at its edges, with 0.20 m of internal height, a 1.50 m length, and a 1.20 m width. Galvanized steel plates were used to make the walls of the solar collector. The galvanized steel plates were painted in grey, and the system was thermally insulated by using wool glass. The drying chamber was 0.90 m long, 1.20 m wide, and 0.96 m in height. An auxiliary heating system was installed on the lower part of the drying chamber to facilitate solar heating. Twenty incandescent lamps of 100 W were used in the auxiliary heating system. The dry air was present due to the dryer, and a chimney was installed with a diameter of 0.20 m; the diameter was measured on the topmost part of the dryer. The drying chamber was composed of eight trays (0.74 m × 0.52 m). These trays were placed inside the drying chamber which had a

total area of 3.08 m². Two doors were located on the back of the system for the introduction and removal of products. The temperature of airflow at the outlet of the proposed system was controlled by a thermostat. Drying banana slices was performed. The banana slices were exposed in an open sun drying hybrid dryer and in the artificial dryer. The obtained drying curves were compared with one another.

The obtained results showed that the time taken by the samples to reach the desired moisture content was lower in the hybrid dryer compared with the artificial dryer and drying that occurred as a result of the natural sun at similar outlet air temperatures. The introduction of incandescent lamps as an auxiliary energy system increases the drying rate in the hybrid dryer. Moreover, the thermal losses were more prominent, and the drying of crops was not homogenous. The drying rate was faster when the crops in the trays were closer to the lamp. The proposed dryer was economically and technically feasible compared with the artificial dryers. This may be presented as a suitable alternative with which to dry crops [109].

Tuncer et al. (2020) worked on a quadruple-pass solar air collector that was installed to a greenhouse dryer. The floor was painted matt-black and built using metal. The quadruple-pass solar air collector was tilted to a 32° angle on a platform. The results showed that by integrating the QPSAC into the dryer, the rate of drying is reduced and performance is improved. It was also observed that the thermal efficiency of the quadruple-pass solar air collector greenhouse dryer was increased by the increase in air mass flow [110].

Azaizia et al. (2020) worked on a PCM and a solar air heater that was installed onto a greenhouse dryer with a mixed mode type of operation. Regarding the results, the drying period was significantly reduced as a result of using the PCM (Phase Change Material) as thermal storage. During the nighttime, the dryer air temperature was higher compared with all other drying processes. The efficiency of the dryer was improved by using Phase Change Materials [15].

To understand the flow and thermal pattern of a solar air heater Khanlari et al. (2020) modelled a tube type solar air heater and analyzed the performance using Ansys Fluent software. The tube is structured as a helix comprising sheet metal. The floor of the dryer and the helical tube is painted matt black. At three different air flow rates, with T-SAH (Tube type solar air heater), and without the tube type solar air heater, these factors comprised two modes used for the operations conducted in this experiment. The drying period was reduced by nearly 30% with the use of T-SAH. A higher performance is achieved by using T-SAH in the dryer [86].

Amer et al. (2010) had undertaken a performance evaluation of a hybrid solar dryer when drying bananas. Direct solar energy and a heat exchanger were used in the development of the hybrid solar dryer. The solar dryer consisted of a drying chamber, a solar collector, a heat exchanger, and a reflector. The dryer operated as a normal solar dryer during regular sunny days and as a hybrid solar dryer during cloudy days. The heat energy was stored in water during sunny periods; moreover, the electric heaters were placed in the water tank. The dryer was used to undertake drying during the night. The efficiency of the dryer increased by recycling around 65% of the drying air. The air temperature rose to 30 to 40 °C above the ambient temperature, so that it was comparable to Mid-European summer conditions. The dryer was capable of drying about 30 kg of banana slices. The dryer required 8 h to achieve its final moisture content, which was 18% of the initial moisture content; the initial moisture content was 82% on a normal sunny day in open sun conditions, and it was reduced by up to 62% when tested later the same day. The physical parameters, such as color, odor, and texture were improved during solar drying compared with open sun drying. Recycling approximately 65% of the air was carried out in order to improve the efficiency of the solar dryer. The use of solar reflectors with holders that move it according to the movement of sun's angle during sunny periods was found to be the most favorable method for collecting solar energy during the daytime. The proposed solar dryer can be used with a supplementary heat source in adverse weather conditions, such as on cloudy days. During sunny periods, approximately 16 °C can be stored in water

by using the solar dryer in the water tank. The heat energy stored inside the dryer can be used during the night in order to transfer the heat from the water to the outside air, thus maintaining air temperature. The color, odor, and texture of the solar-dried crops were better when compared with open sun-dried crops. The cashew nuts were selected for drying; this is one of the most energy-intensive processes in the processing industry [111].

Brarnwal and Tiwari (2011) examined the convective heat transfer coefficient of a hybrid photovoltaic thermal (PVT) greenhouse dryer. The drying capacity of the dryer was 100 kg. Thompson seedless grapes were selected for drying under open sun conditions and they were placed in a forced convection greenhouse dryer. The Thompson grapes were classified as grade I and II. Grade I grapes were raw, green, and premature, and Grade II grapes were yellowish and fully matured. In April 2017, the experiment was performed to measure the convective heat transfer coefficient. Various parameters such as the ambient air temperature, the grapes' surface temperature, the ambient humidity, the moisture evaporated, the greenhouse air temperature, and the green house humidity, were taken in order to conduct the experiment. The value of the convective heat transfer coefficient for the sample in Group I lay between 0.26 and 0.31 W/m²·K. Moreover, regarding open sun conditions, it lay between 0.34 and 0.40 W/m²·K. For Group II grapes, the value of the convective heat transfer coefficient lay between 0.45 and 1.21 W/m²·K. Regarding open sun conditions, it lay between 0.46 and 0.97 W/m²·K, respectively [112].

Okoroigwe et al. (2013) developed a solar and biomass dryer for underdeveloped countries. A demonstration model was composed of a combination solar and biomass dryer with three equally spaced trays. Fresh yam chips were used as the testing materials for a period of four days. The results obtained were satisfactory and suitable for optimization purposes. During the test period, though the ambient temperature was between 24 and 30 °C, the maximum tray temperature was measured as 53 °C, in combination with solar and biomass heating sources. The combination solar and biomass dryer provided an optimal drying rate of 0.0142 kg/h. This drying rate is higher than biomass drying and solar drying alone (i.e., 0.0032 kg/h and 0.00732 kg/h); therefore, this shows that using a combination solar and biomass dryer is more efficient than using these two dryers individually [113].

Reyes et al. (2014) introduced a hybrid solar drying system for drying tomatoes. In the hybrid solar dryer, tomato pieces were dehydrated with the help of a solar panel with an area of 3 m² and electric resistances. Approximately 80–90% of the air was recycled in the outlet of the tray. The air temperature was managed between 50 to 60 °C in the tray of the dryer. The air temperature rose between 5 and 18 °C at the outlet of the tray. The critical moisture content was significantly affected by the sample size and temperature. The dehydrated tomatoes indicated a notorious redness in terms of the colour parameter, and the rehydration state was reached within a minimum time of 50 min. With the help of three empirical models, the drying kinetics were regulated. The Guggenheim–Anderson, De Boer, and Peleg models were applied to adjust the Sorption isotherms. The solar energy input resulted in a 6.6–12.5% energy saving [114].

Aritesty and Wulandani (2014) studied the drying process of wild ginger slices by using the solar greenhouse dryer (rack type). For regulating the drying temperature inside the dryer, during the night, biomass energy was supplied. As a result of the biomass energy provision, the drying period was reduced, and the performance of the dryer was improved. The drying efficiency was increased as a result of the drying capacity increasing [115].

Sajith and Muraleedharan (2014) conducted a study on the performance of a solar hybrid dryer involved in drying Alma. Alma is a fruit that has a high content of Vitamin C. The hybrid solar dryer in the proposed model was assisted by a PV system. This system was arranged in such a way that both electric energy and thermal energy were produced simultaneously. The hybrid system provided a better performance in comparison with traditional drying techniques. The structure of the system aimed to help protect crops from damage such as microbial contamination [116].

Dhanushkodi et al. (2014) developed a hybrid solar dryer for drying cashew nuts. It consisted of a solar flat plate collector, a drying chamber, and a biomass heater. The

40 kg of cashew nuts used in the experiment had an initial moisture content of 9%. The test was carried out using two modes of operation: hybrid natural convection and hybrid forced convection. Regarding the abovementioned two modes, the drying efficiency and drying time were compared with the solar drying method. The system attained a drying temperature between 50 to 70 °C. Within 7 h, the required moisture content of 3% was achieved, and the system efficiency was estimated to be 5.08%. In the case of hybrid natural drying, the moisture content needed was achieved in 9 h, and the average system efficiency was obtained as being 3.17%. During the drying process, the fuel consumption was 0.5 kg/h for the forced mode and 0.75 kg/h for the natural mode. The hybrid force mode is more effective in drying products when compared with open sun drying. The dryer can be operated in many different climatic conditions, for example: as a hybrid dryer on a cloudy day, as a solar dryer on regular sunny days, and as a biomass dryer during the night. Based on the research so far, it can be posited that the hybrid dryer developed by the authors is sufficient for drying cashew nuts in the rural areas of underdeveloped countries. The solar biomass dryer has been developed for drying 40 kg of cashew nuts per batch. The hybrid forced mode has an average collector efficiency of 75.6%, and the temperature ranges between 55 to 75 °C. The strength of the collector efficiency and temperature range depends on the fuel used and the climatic conditions in the area. This technology can also be used suitably when drying other agricultural products. The products obtained are of a high quality and the drying time is almost half of that of the open sun drying method [117].

Vengsungnle et al. (2020) developed the automatic closed loop control system integrated with a conventional greenhouse dryer. The PV (photovoltaic) and electric heater was attached onto the dryer. The study was conducted during the winter season and a cover was made of a clear plastic film on the dryer, which worked as greenhouse cover. To regulate the relative humidity difference in the dryer, based on the inside and outside air limitations, the fans were operated according to the requirements of the system. The results show that the drying time was reduced significantly by maintaining a controlled frequency level in the dryer with regard to temperature and ventilation. In this experiment, the initial investment is very high compared with open sun drying due to the electric equipment being used and the high energy cost, as the dryer was equipped with the control system (automated) [118].

Lakshmi et al. (2018) developed an integrated mixed mode solar dryer with paraffin wax which operated under forced convection conditions for drying sliced black turmeric. The drying chamber was equipped with two solar air heaters so that it would be similar to a hybrid dryer. It contained six trays and a blower, a shell, a tube heat exchanger, and paraffin wax. In comparison with open sun drying, the system saved time by up to 60.7% [34].

The use of PCM as a thermal storage unit in solar greenhouse crop drying has been rarely researched in the literature. The current study contributes to the research on this new drying method, which is a solar greenhouse dryer that contains paraffin wax as a latent heat storage material. During periods that are less sunny, supplemental energy sources are used to maintain the drying process. A comparison of various types of hybrid greenhouse dryers has been illustrated in Table 3.

Table 3 shows that the hybrid greenhouse dryer enhanced the drying efficiency, protected the products from damage in terms of nutrient content, and it reduced the drying time. It also enhanced the operational time of the dryer.

Table 3. Comparison of various types of hybrid greenhouse dryer.

Authors [Ref.]	Year	Types of Hybrid Dryer	Results/Significant Findings
Bassey [119]	1986	Hybrid Sawdust–Solar Dryer	A “hole-through-sawdust” burner generates steam through the use of a heat exchanger and direct solar energy. According to test results utilizing okra under no-load conditions, a dryer operating between 40–70 °C may dry items twice as quickly as the conventional approach.
Ferreira et al. [109]	2007	Hybrid Solar–Electrical Dryer	A hybrid solar-electrical dryer with two chambers—a solar chamber and a drying chamber with an air heater—was examined. The device’s airflow was evaluated experimentally, and the average values of the temperature and mass flow were reported as functions of the surrounding environment.
Nandwani [120]	2007	Hybrid Solar–Food Processor	A hybrid food processor that serves many functions was created, and its different technical and usable elements were researched. Cooking, pasteurizing water, distilling small amounts of water (to remove various minerals), and drying household goods (fruits, vegetables, condiments/herbs, etc.) were activities that were undertaken using this processor.
Boughali et al. [121]	2009	Hybrid Solar–Electrical Dryer	The study was conducted in a newly designed air drying passage at a mass flow rate that ranged between 0.04 and 0.08 kg/m ² s, which is a relatively high range. Most researchers did not adequately study this spectrum.
Amer et al. [111]	2010	New Hybrid Solar Dryer with Heat Exchanger	A hybrid solar dryer was conceived and built using a heat exchanger and direct solar energy. The dryer was used as a solar dryer on typical sunny days and as a hybrid solar dryer on cloudy days. With the help of electric heaters placed in the water tank, and the heat energy that was saved in the water during the day, drying was also able to occur at night. By reusing around 65% of the drying air within the solar dryer, and by expelling a little portion of it outdoors, the dryer’s efficiency was increased.
Hossain et al. [30]	2010	Hybrid Solar Dryer with FPC	A hybrid solar dryer prototype was created for tomato drying. It was made up of a drying unit, heat storage with an auxiliary heating unit, and a flat-plate concentrating collector. The dryer was tested in a variety of climatic and operational circumstances.
Reyes et al. [122]	2013	Hybrid Solar Electric Dryer	A hybrid solar dryer equipped with electric resistances and a 3 m ² solar panel was used for mushroom drying. SCD Model was used to estimate the effective diffusivity given that the R ² value was greater than 0.98, in accordance with the literature.
Reyes et al. [114]	2014	Hybrid Solar Dryer with electric resistance and Paraffin wax	Three empirical models allowed for an adequate adjustment of drying kinetics. The Guggenheim–Anderson–de Boer and Peleg models provide reliable adjustments for the sorption isotherms. Energy was saved in the range of 6.6–12.5% as a result of the solar energy intake.
Okoroigwe et al. [113]	2015	Solar–Biomass Hybrid Dryer	The heat exchanger and back pass solar collector improved the tray temperature during no-load conditions.
Yassen and Al-Kayiem [123]	2016	Hybrid Solar/Thermal Dryer	Experimental research was conducted in order to determine whether the hybrid solar-thermal drying system with a recovery dryer would perform better than the system without recovery. The investigations were carried out in two operational modes for drying red chili: thermal mode and hybrid mode.
Eltawil et al. [124]	2018	Hybrid Solar PV Tunnel Dryer With Solar Collector	Results showed that the designed dryer required 210 to 360 min to dry peppermint, but open-air sun drying required 270 to 420 min.
Amer et al. [125]	2018	Hybrid Solar Dryer Coupled With Electric Air Heater	For a better drying performance, the dryer was connected to an electric air heater with auto control and a blackened absorber surface. Ginger was dried using the natural convection mode.

Table 3. Cont.

Authors [Ref.]	Year	Types of Hybrid Dryer	Results/Significant Findings
Poonia et al. [126]	2018	PV/T Hybrid Solar Dryer	The root mean square error (RMSE), coefficient of determination (R ²), and reduced chi-square (2) between the observed and estimated MR was used to compare the drying models' performance.
Amjad et al. [91]	2020	Solar–Gas Hybrid Dryer	A thorough thermal analysis (based on energy and exergy) was carried out on a newly created inline airflow solar hybrid dryer (coupled with a gas burner and solar evacuated tube collector). Green chilies were used in the studies, and they were heated to 60 °C using three different heating sources: dual source (gas and solar), gas, and solar.
Hao et al. [127]	2020	New Hybrid Solar Dryer coupled with FPSC and DF-FPSC	By using various operation strategies, the novel hybrid solar dryer application can regulate the air temperature in the drying chamber within a desirable range. By contrasting open sun drying with the hybrid solar dryer, drying trials for lemon slices were carried out (OSD).

8.4. Studies Conducted on Environmental Aspects of Greenhouse Dryers

Environmental analyses give details on the damaging consequences that dryer emissions have on the environment. To evaluate the impacts of the dryers in terms of CO₂ emissions, embodied energy, carbon credits earned, and net CO₂ that is mitigated, some important parameters need to be determined.

Ayyappan (2018) evaluated the performance of a hybrid solar–biomass dryer for drying dry coconuts in two parts. The hybrid solar–biomass dryer performed well compared with open sun drying by reducing the drying rate. It was discovered that the dryer had a long cost payback period and it produced considerable CO₂ emissions. The dryer's embodied energy was determined to be 18,302 kWh [128].

Motevali and Kolor (2017) examined the energy consumption of infrared, hot air, hot air microwaves, hybrid hot air infrared microwaves, hybrid photovoltaic–thermal solar dryers, vacuums, and emission of greenhouse gases (GHG) into the atmosphere. The energy consumption and GHG emissions are lowest for microwave dryers out of all the dryers. The source of electricity generation and the GHG emissions should also be considered in relation to its productive activities. The expansion of the microwave dryer was hampered by factors including uneven heating, deteriorating food textures, and so on. Based on the results, except for the microwave dryer, the PVT solar dryer showed reduced GHG emissions in comparison to a conventional dryer [129].

Saini et al. (2017) analyzed a solar greenhouse dryer combined with various photovoltaic technologies such as p-Si, c-Si, CdTe, a-Si, and CIGS. The experiment operated under active conditions. According to the data, CIGS has the lowest and c-Si has the greatest levels of CO₂ emission (in kg), but c-Si technology allows for the highest net level of CO₂ to be mitigated (in tons) and carbon credits to be earned (in USD). The c-Si is the best option in terms of producing energy [130].

Nayak et al. (2011) evaluated a greenhouse dryer that was a hybrid photovoltaic–thermal dryer that was used for drying mint leaves. The efficiency of the dryer was determined to be 34.2% and the dryer reduced the drying time of mint when compared with open sun drying conditions. The CO₂ that would be mitigated over the lifetime of the dryer was calculated to be 140.97 tons. The carbon credit earned per ton ranged between USD 704.85 and USD 2819.40 [131].

Economic analyses play an important role in solar greenhouse dryer usage. They help determine how feasible it is to use a solar greenhouse from an economic standpoint [132,133]. An economic analysis helps to determine the cost of a product in any commercial production. The annualized cost method is mainly used to determine the economic parameters of the dryer. NPV, ROI, drying cost/kg, payback period, and so on, are some of the important parameters used in such an evaluation.

Barnwal and Tiwari (2008) determined the parameters of the economic factors relating to greenhouse dryers (hybrid PV/T) for grapes [134]. The results showed that the cost of drying/kg and the payback period was reduced. The payback period and drying cost/kg increases with the increase in the number of clear sunny days. The annualized cost method was used for the calculation of payback period. The ROI and initial investment were the important economic factors used to evaluate the NPV. The consequences are in accordance with existing findings [135–137].

Khadraoui and Bouadila (2020) evaluated the economic and performance-based aspects of a chapel-shaped greenhouse dryer [138]. The dryer was installed with a flat plate collector. Compared with the open sun drying process, this process yields a higher drying rate and it reduced the drying time by 7 h. As a result, the payback period was calculated as being 1.02 years. This payback period is less than the payback periods of other existing dryers and the same findings have unveiled by Guo et al. (2022) [139].

Chauhan et al. (2019) worked on a solar air heater that was integrated with an opaque and insulated north wall greenhouse dryer. At bottom of the dryer, a solar air heater was used to dry flakes of bitter melon. This dryer was found to be effective in terms of energy analysis and it was also found to be environmentally friendly when drying agricultural products [140,141].

9. Challenges and Opportunities

This discussion shows that greenhouse drying could be an effective solution to the problems posed by the enormity of crop production. Indeed, it is a method which requires less drying time for crops after they have been harvested. The major shortcoming of greenhouse dryers is the development of moisture gradients during the drying process; therefore, the ongoing study undertaken by researchers on the effects of greenhouse drying on crop quality requires more research that focuses mainly on product quality. The following topics could be studied in future research concerning crop drying with greenhouse dryers:

- i. The maximum acceptable temperature needs to be determined without compromising the quality of the dried crop. Hence analyzing the optimum drying air temperature is needed when drying crops.
- ii. The proper utilization of moist air needs to occur in order to decrease the relative humidity and increase the drying rate.
- iii. The energy and exergy efficiencies should be analyzed properly as the present research is limited with regard to greenhouse dryers.
- iv. The comprehensive numerical models for the greenhouse drying of crops are needed to be developed as they include changes to the moisture on the surface.

10. Final Remarks and Conclusions

This paper offers a thorough analysis of greenhouse dryers produced for drying a variety of agricultural goods based on geometrical characteristics, geographical location, and mode of operation. It also discusses thermal modelling methodologies and environmental aspects. Additionally, a brief discussion notes the evaluation of the dryers' performances when integrated with thermal energy storage systems and PV panels. The review's executive summary is as follows:

- The choice of solar greenhouse dryer varies according to region, and generalizing it to a specific orientation and shape is not possible. Among the numerous shapes explored in greenhouse dryer design, Quonset and even span types are commonly utilized globally, with the even span being favored since it receives more solar radiation in all seasons. When compared with other orientations, the east–west direction is chosen because of its lower energy requirements for heating and cooling as well as its capacity to absorb more solar radiation into the dryer. Commonly utilized as cladding materials are low-density polyethylene films that are stabilized with ultraviolet, infrared, and anti-drop technology.

- A combination of latent heat storage and sensible heat storage units in the greenhouse dryer can be employed to attain the constant drying of products in all seasons. In this situation, the greenhouse dryer can be equipped with a black-painted gravel bed and a PCM (paraffin wax). Use of a heat exchanger and heat pump can be used for providing additional heat to the greenhouse at lower ambient temperatures.
- On the basis of different statistical parameters (reduced chi-square, root mean square error, and mean absolute error) the different drying models (thin layer) that are available in the literature are compared and confirmed with the data of experimental drying curves. The study provides a thorough investigation of the several thin layer models that are available, and the best-fitting models are listed, based on the type of dryer, how it operates, and the goods (fruits, vegetables, and spices). It is also based on the mode of operation, product, location, and kind of greenhouse dryer. This description can be used as a reference tool for choosing an appropriate thin layer model. As a result, it is challenging to characterize the drying behavior using a single thin layer model of a product, and it is almost impossible to construct a generic thin layer model.

Agricultural land is being turned into commercial structures, and hence, it is lost to urban expansion as the world's population continues to grow. As a result, there is a pressing need to develop a cost-effective technology that is best suited to local surroundings in order to improve the greenhouse dryer business. Greenhouse drying, a unique process for drying food and agricultural produce, could be used to reduce post-harvest losses and improve the quality of a variety of items. Greenhouse dryers are utilized for agricultural cultivation, solar stills, biogas, and fishpond systems, according to the literature review. Greenhouse benefits include increased crop yields (15–17%), high reliability, the ability to cultivate vegetables and fruit crops outside of the growing season, better quality dried products, lower drying losses, and a controlled environment for crop cultivation, solar stills, biogas production, and more.

The heat and mass transfer analyses of several greenhouse solar dryers created by diverse researchers are presented in this paper. This review aids the researcher in obtaining a better understanding of the heat and mass movement that occurs inside the greenhouse dryer, as well as how it might be enhanced.

11. Recommendations and Future Scope of Research

A substantial amount of scientific work on solar greenhouse dryers created for drying a variety of agricultural goods is summarised. Considering the literature review, the present investigation of the proposed heat storage-based hybrid greenhouse dryer can be extended as per the following ways:

- (a) A thorough experimental investigation is required to investigate the feasibility of building a combined thermal storage unit (latent heat and sensible) used in the greenhouse dryer in order to capitalize on a higher specific heat capacity and cost effectiveness. To avoid overuse of thermal storage elements, the ideal thickness of the latent heat storage and sensible heat storage system must be estimated in advance.
- (b) The thermal performance of the hybrid greenhouse dryer can be investigated at different mass flow rates and porosity values.
- (c) The thermal performance of the proposed system can be investigated by recirculation of exhaust air inside the drying chamber.
- (d) The solar air heater can be modified with heat storage-based material such as PCM and performance analysis can be done.
- (e) The CFD analysis of the proposed system can be conducted and compared with other investigators.
- (f) The thermal performance of the proposed hybrid greenhouse dryer can be further investigated by varying the packed bed materials and porosity values.
- (g) A complete experimental and simulation analysis on the thin-layer model must be performed, taking into account characteristics such as the dryer's boundary conditions,

the product's shrinkage behaviour, the equilibrium moisture content, time-varying and diffusivity parameters such as the uncertainty values, and temperature; these have an impact during the drying rate measurements. These assumptions need to be taken into account when creating of future thin-layer models. This will contribute to improving the predictability of product drying behavior.

Author Contributions: Conceptualization, A.A., O.P., A.K., R.C., S.S., V.K., K.K. and C.L.; formal analysis, A.A., O.P., A.K., R.C., S.S., V.K., K.K. and C.L.; investigation, A.A., O.P., A.K., R.C., S.S., V.K. and C.L.; writing—original draft preparation, A.A., O.P., A.K., R.C., S.S., V.K., K.K. and C.L.; writing—review and editing, S.S. and E.M.T.E.; supervision, S.S. and E.M.T.E.; project administration, S.S. and E.M.T.E.; funding acquisition, S.S. and E.M.T.E. All authors have read and agreed to the published version of the manuscript.

Funding: This research received no external funding.

Institutional Review Board Statement: Not applicable.

Informed Consent Statement: Not applicable.

Data Availability Statement: Not applicable.

Conflicts of Interest: The authors declare no conflict of interest.

References

- Sharma, N.; Garcha, S.; Singh, S. Potential of *Lactococcus lactis* subsp. *lactis* MTCC 3041 as a biopreservative. *J. Microbiol. Biotechnol. Food Sci.* **2019**, *2019*, 168–171.
- Singh, S.; Kumar, S. Testing method for thermal performance-based rating of various solar dryer designs. *Sol. Energy* **2012**, *86*, 87–98. [[CrossRef](#)]
- Ayres, R.U.; Walter, J. The greenhouse effect: Damages, costs and abatement. *Environ. Resour. Econ.* **1991**, *1*, 237–270. [[CrossRef](#)]
- Kumar, M.; Kumar, A. Performance assessment and degradation analysis of solar photovoltaic technologies: A review. *Renew. Sustain. Energy Rev.* **2017**, *78*, 554–587. [[CrossRef](#)]
- Supranto Sopian, K.; Daud, W.; Othman, M.; Yatim, B. Design of an experimental solar assisted dryer for palm oil fronds. *Renew. Energy* **1999**, *16*, 643–646. [[CrossRef](#)]
- Belessiotis, V.; Delyannis, E. Solar drying. *Sol. Energy* **2011**, *85*, 1665–1691. [[CrossRef](#)]
- Bahammou, Y.; Tagnamas, Z.; Lamharrar, A.; Idliman, A. Thin-layer solar drying characteristics of Moroccan horehound leaves (*Marrubium vulgare* L.) under natural and forced convection solar drying. *Sol. Energy* **2019**, *188*, 958–969. [[CrossRef](#)]
- Essalhi, H.; Benchrifa, M.; Tadili, R.; Bargach, M.N. Experimental and theoretical analysis of drying grapes under an indirect solar dryer and in open sun. *Innov. Food Sci. Emerg. Technol.* **2018**, *49*, 58–64. [[CrossRef](#)]
- Sharma, A.; Chen, C.R.; Lan, N.V. Solar-energy drying systems: A review. *Renew. Sustain. Energy Rev.* **2009**, *13*, 1185–1210. [[CrossRef](#)]
- Kumar, A.; Rai, A.K. Comparative Study of Open Sun Drying & Solar Cabinet Drying Techniques for Drying of Green Chilies. *Int. J. Prod. Technol. Manag.* **2016**, *7*, 18–26.
- Sahdev, R.K.; Kumar, M.; Dhingra, A.K. A comprehensive review of greenhouse shapes and its applications. *Front. Energy* **2017**, *13*, 427–438. [[CrossRef](#)]
- Téllez, M.C.; Figueroa, I.P.; Castillo-Téllez, B.; Vidaña, E.C.L.; López-Ortiz, A. Solar drying of Stevia (Rebaudiana Bertoni) leaves using direct and indirect technologies. *Sol. Energy* **2018**, *159*, 898–907. [[CrossRef](#)]
- Dissa, A.; Bathiebo, J.; Kam, S.; Savadogo, P.; Desmorieux, H.; Koulidiati, J. Modelling and experimental validation of thin layer indirect solar drying of mango slices. *Renew. Energy* **2009**, *34*, 1000–1008. [[CrossRef](#)]
- Bala, B.K.; Woods, J.L. Simulation of the indirect natural convection solar drying of rough rice. *Sol. Energy* **1994**, *53*, 259–266. [[CrossRef](#)]
- Azaizia, Z.; Kooli, S.; Hamdi, I.; Elkhali, W.; Guizani, A.A. Experimental study of a new mixed mode solar greenhouse drying system with and without thermal energy storage for pepper. *Renew. Energy* **2020**, *145*, 1972–1984. [[CrossRef](#)]
- Prakash, O.; Kumar, A. Environmental Analysis and Mathematical Modelling for Tomato Flakes Drying in a Modified Greenhouse Dryer under Active Mode. *Int. J. Food Eng.* **2014**, *10*, 669–681. [[CrossRef](#)]
- Galliou, F.; Markakis, N.; Fountoulakis, M.; Nikolaidis, N.; Manios, T. Production of organic fertilizer from olive mill wastewater by combining solar greenhouse drying and composting. *Waste Manag.* **2018**, *75*, 305–311. [[CrossRef](#)]
- Patil, R.; Gawande, R. A review on solar tunnel greenhouse drying system. *Renew. Sustain. Energy Rev.* **2016**, *56*, 196–214. [[CrossRef](#)]
- Maraveas, C. Environmental sustainability of greenhouse covering materials. *Sustainability* **2019**, *11*, 6129. [[CrossRef](#)]
- Çerçi, K.N.; Daş, M. Modeling of Heat Transfer Coefficient in Solar Greenhouse Type Drying Systems. *Sustainability* **2019**, *11*, 5127. [[CrossRef](#)]

21. Jain, D.; Tiwari, G.N. Modeling and optimal design of evaporative cooling system in controlled environment greenhouse. *Energy Convers. Manag.* **2002**, *43*, 2235–2250. [[CrossRef](#)]
22. Tiwari, S.; Agrawal, S.; Tiwari, G. PVT air collector integrated greenhouse dryers. *Renew. Sustain. Energy Rev.* **2018**, *90*, 142–159. [[CrossRef](#)]
23. Condori, M.; Echazú, R.; Saravia, L. Solar drying of sweet pepper and garlic using the tunnel greenhouse drier. *Renew. Energy* **2001**, *22*, 447–460. [[CrossRef](#)]
24. Khawale, V.R.; Khawale, R.P. Performance Evaluation of a double pass Indirect Solar Drier for drying of Red Chili. *Sol. Energy* **2016**, *3*, 514–518.
25. Dhanore, R.T.; Jibhakate, Y.M. A solar tunnel dryer for drying red chilly as an agricultural product. *Int. J. Eng. Res. Technol.* **2014**, *3*, 310–314.
26. Fudholi, A.; Othman, M.Y.; Ruslan, M.H.; Sopian, K. Drying of Malaysian *Capsicum annum* L. (Red Chili) Dried by Open and Solar Drying. *Int. J. Photoenergy* **2013**, *2013*, 167895. [[CrossRef](#)]
27. Kaewkiew, J.; Nabnean, S.; Janjai, S. Experimental investigation of the performance of a large-scale greenhouse type solar dryer for drying chilli in Thailand. *Procedia Eng.* **2012**, *32*, 433–439. [[CrossRef](#)]
28. Banout, J.; Ehl, P.; Havlik, J.; Lojka, B.; Polesny, Z.; Verner, V. Design and performance evaluation of a Double-pass solar drier for drying of red chilli (*Capsicum annum* L.). *Sol. Energy* **2011**, *85*, 506–515. [[CrossRef](#)]
29. Mohanraj, M.; Chandrasekar, P. Performance of a forced convection solar drier integrated with gravel as heat storage material for chili drying. *J. Eng. Sci. Technol.* **2009**, *4*, 305–314.
30. Hossain, M.A.; Amer, B.M.A.; Gottschalk, K. Hybrid solar dryer for quality dried tomato. *Dry. Technol.* **2008**, *26*, 1591–1601. [[CrossRef](#)]
31. Karthikeyan, A.K.; Murugavelh, S. Thin layer drying kinetics and exergy analysis of turmeric (*Curcuma longa*) in a mixed mode forced convection solar tunnel dryer. *Renew. Energy* **2018**, *128*, 305–312. [[CrossRef](#)]
32. Borah, A.; Hazarika, K.; Khayer, S.M. Drying kinetics of whole and sliced turmeric rhizomes (*Curcuma longa* L.) in a solar conduction dryer. *Inf. Process. Agric.* **2015**, *2*, 85–92. [[CrossRef](#)]
33. Gunasekar, J.J.; Kaleemullah, S.; Doraisamy, P.; Kamaraj, S. Evaluation of solar drying for post harvest curing of turmeric (*Curcuma longa* L.). *AMA Agric. Mech. Asia Africa Lat. Am.* **2006**, *37*, 9–13.
34. Lakshmi, D.; Kumar, M.P.; Layek, A.; Nayak, P.K. Drying kinetics and quality analysis of black turmeric (*Curcuma caesia*) drying in a mixed mode forced convection solar dryer integrated with thermal energy storage. *Renew. Energy* **2018**, *120*, 23–34. [[CrossRef](#)]
35. Yahya, M. Performance analysis of solar drying system using double pass solar air collector with finned absorber for drying copra. *Contemp. Eng. Sci.* **2018**, *11*, 523–536. [[CrossRef](#)]
36. Ayyappan, S.; Mayilsamy, K. Experimental investigation on a solar tunnel drier for copra drying. *J. Sci. Ind. Res.* **2010**, *69*, 635–638.
37. Mohanraj, M.; Chandrasekar, P. Drying of copra in a forced convection solar drier. *Biosyst. Eng.* **2008**, *99*, 604–607. [[CrossRef](#)]
38. Hamdi, I.; Kooli, S.; Elkhadraoui, A.; Azaizia, Z.; Abdelhamid, F.; Guizani, A. Experimental study and numerical modeling for drying grapes under solar greenhouse. *Renew. Energy* **2018**, *127*, 936–946. [[CrossRef](#)]
39. Ramos, I.N.; Brandão, T.R.; Silva, C.L. Simulation of solar drying of grapes using an integrated heat and mass transfer model. *Renew. Energy* **2015**, *81*, 896–902. [[CrossRef](#)]
40. Rathore, N.S.; Panwar, N.L. Experimental studies on hemi cylindrical walk-in type solar tunnel dryer for grape drying. *Appl. Energy* **2010**, *87*, 2764–2767. [[CrossRef](#)]
41. Fadhel, A.; Kooli, S.; Farhat, A.; Bellghith, A. Study of the solar drying of grapes by three different processes. *Desalination* **2005**, *185*, 535–541. [[CrossRef](#)]
42. Yaldiz, O.; Ertekin, C.; Uzun, H.I. Mathematical modeling of thin layer solar drying of sultana grapes. *Energy* **2001**, *26*, 457–465. [[CrossRef](#)]
43. Akoto, E.Y.; Klu, Y.A.; Lamptey, M.; Asibuo, J.Y.; Heflin, M.; Phillips, R.; Jordan, D.; Rhoads, J.; Hoisington, D.; Chen, J. Solar Drying: A Means of Improving the Quality of Peanuts in Ghana. *Peanut Sci.* **2018**, *45*, 56–66. [[CrossRef](#)]
44. Noomhorm, A.; Kumar, P.K.; Sabarez, H.T. Design and development of a conduction drier for accelerated drying of peanuts. *J. Food Eng.* **1994**, *21*, 411–419. [[CrossRef](#)]
45. Bunn, J.M.; Henson, W.H., Jr.; Walton, L.R. Drying equation for high moisture materials. *J. Agric. Eng. Res.* **1972**, *17*, 343–347. [[CrossRef](#)]
46. Abdulmajid, A.M. An alternative to Open-Sun Drying of Silver Cyprinid (*Rastrineobola argentea*) Fish Under Varying Climatic Condition in Kenya. *Int. Sch. J.* **2015**, *3*, 298–312.
47. Basunia, M.A.; Al-Handali, H.H.; Al-Balushi, M.I.; Mahgoub, O. Drying of Fish Sardines in Oman Using Solar Tunnel Dryers. *J. Agric. Sci. Technol.* **2011**, *1*, 108–114.
48. Bhor, P.P.; Khandetod, Y.P.; Mohod, A.G.; Sengar, S.H. Performance study of solar tunnel dryer for drying of fish variety Dhoma. *Int. J. Agric. Eng.* **2009**, *2*, 222–227.
49. Chauhan, P.S.; Kumar, A. Heat transfer analysis of north wall insulated greenhouse dryer under natural convection mode. *Energy* **2017**, *118*, 1264–1274. [[CrossRef](#)]
50. Prakash, O.; Kumar, A. Thermal performance evaluation of modified active greenhouse dryer. *J. Build. Phys.* **2013**, *37*, 395–402. [[CrossRef](#)]

51. Jain, D.; Tiwari, G. Effect of greenhouse on crop drying under natural and forced convection II. Thermal modeling and experimental validation. *Energy Convers. Manag.* **2004**, *45*, 2777–2793. [\[CrossRef\]](#)
52. Ahmad, A.; Prakash, O. Thermal analysis of north wall insulated greenhouse dryer at different bed conditions operating under natural convection mode. *Environ. Prog. Sustain. Energy* **2019**, *38*, e13257. [\[CrossRef\]](#)
53. Balasuadhakar, A.; Fisseha, T.; Atenafu, A.; Bino, B. A review on passive solar dryers for agricultural products. *Int. J. Innov. Res. Sci. Technol.* **2016**, *3*, 64–70.
54. Ahmad, A.; Prakash, O. Performance evaluation of a solar greenhouse dryer at different bed conditions under passive mode. *J. Sol. Energy Eng.* **2020**, *142*, 011006. [\[CrossRef\]](#)
55. Sahu, T.K.; Gupta, V.; Singh, A.K. Experimental Analysis of Open, Simple and Modified Greenhouse Dryers for Drying Potato Flakes under Forced Convection. *Int. J. Eng. Res. Appl.* **2016**, *6*, 56–60.
56. Rabha, D.K.; Kumar, M.P.; Somayaji, C. Experimental investigation of thin layer drying kinetics of ghost chilli pepper (*Capsicum chinense* Jacq.) dried in a forced convection solar tunnel dryer. *Renew. Energy* **2017**, *105*, 583–589. [\[CrossRef\]](#)
57. Jin, W.; Mujumdar, A.S.; Zhang, M.; Shi, W. Novel Drying Techniques for Spices and Herbs: A Review. *Food Eng. Rev.* **2017**, *10*, 34–45. [\[CrossRef\]](#)
58. Condori, M.; Saravia, L. The performance of forced convection greenhouse driers. *Renew. Energy* **1998**, *13*, 453–469. [\[CrossRef\]](#)
59. Pochont, N.R.; Mohammad, M.N.; Pradeep, B.T.; Kumar, P.V. A comparative study of drying kinetics and quality of Indian red chilli in solar hybrid greenhouse drying and open sun drying. *Mater. Today Proc.* **2020**, *21*, 286–290. [\[CrossRef\]](#)
60. Ahmad, A.; Prakash, O.; Kumar, A. Drying kinetics and economic analysis of bitter melon slices drying inside hybrid greenhouse dryer. *Environ. Sci. Pollut. Res.* **2021**, 1–15. [\[CrossRef\]](#)
61. Dina, S.F.; Ambarita, H.; Napitupulu, F.H.; Kawai, H. Study on effectiveness of continuous solar dryer integrated with desiccant thermal storage for drying cocoa beans. *Case Stud. Therm. Eng.* **2015**, *5*, 32–40. [\[CrossRef\]](#)
62. Jain, D. Determination of Convective Heat and Mass Transfer Coefficients for Solar Drying of Fish. *Biosyst. Eng.* **2006**, *94*, 429–435. [\[CrossRef\]](#)
63. Gupta, R.; Tiwari, G.; Kumar, A.; Gupta, Y. Calculation of total solar fraction for different orientation of greenhouse using 3D-shadow analysis in Auto-CAD. *Energy Build.* **2012**, *47*, 27–34. [\[CrossRef\]](#)
64. Chauhan, P.S.; Kumar, A. Performance analysis of greenhouse dryer by using insulated north-wall under natural convection mode. *Energy Rep.* **2016**, *2*, 107–116. [\[CrossRef\]](#)
65. El-Sebaei, A.; Shalaby, S. Experimental investigation of an indirect-mode forced convection solar dryer for drying thymus and mint. *Energy Convers. Manag.* **2013**, *74*, 109–116. [\[CrossRef\]](#)
66. Chauhan, P.S.; Kumar, A.; Tekasakul, P. Applications of software in solar drying systems: A review. *Renew. Sustain. Energy Rev.* **2015**, *51*, 1326–1337. [\[CrossRef\]](#)
67. Ahmad, A.; Prakash, O. Development of mathematical model for drying of crops under passive greenhouse solar dryer. *Mater. Today Proc.* **2021**, *47*, 6227–6230. [\[CrossRef\]](#)
68. Tiwari, G.N.; Kumar, S.; Prakash, O. Evaluation of convective mass transfer coefficient during drying of jaggery. *J. Food Eng.* **2004**, *63*, 219–227. [\[CrossRef\]](#)
69. Kumar, A.; Tiwari, G. Thermal modeling of a natural convection greenhouse drying system for jaggery: An experimental validation. *Sol. Energy* **2006**, *80*, 1135–1144. [\[CrossRef\]](#)
70. Sacilik, K.; Keskin, R.; Elicin, A.K. Mathematical modelling of solar tunnel drying of thin layer organic tomato. *J. Food Eng.* **2006**, *73*, 231–238. [\[CrossRef\]](#)
71. Janjai, S.; Intawee, P.; Kaewkiew, J.; Sritus, C.; Khamvongsa, V. A large-scale solar greenhouse dryer using polycarbonate cover: Modeling and testing in a tropical environment of Lao People's Democratic Republic. *Renew. Energy* **2011**, *36*, 1053–1062. [\[CrossRef\]](#)
72. Turhan, K. An Investigation on the performance Improvement of greenhouse-type agricultural dryers. *Renew Energy* **2006**, *31*, 1055–1071.
73. Condori, M.; Saravia, L. Analytical model for the performance of the tunnel-type greenhouse dryer. *Renew Energy* **2003**, *28*, 467–485. [\[CrossRef\]](#)
74. Jain, D. Modeling the performance of greenhouse with packed bed thermal storage on crop drying application. *J. Food Eng.* **2005**, *71*, 170–178. [\[CrossRef\]](#)
75. Janjai, S.; Lamlert, N.; Intawee, P.; Mahayothee, B.; Bala, B.; Nagle, M.; Müller, J. Experimental and simulated performance of a PV-ventilated solar greenhouse dryer for drying of peeled longan and banana. *Sol. Energy* **2009**, *83*, 1550–1565. [\[CrossRef\]](#)
76. Panwar, N.L.; Kaushik, S.C.; Kothari, S. Thermal modeling and experimental validation of solar tunnel dryer: A clean energy option for drying surgical cotton. *Int. J. Low-Carbon Technol.* **2013**, *11*, 16–28. [\[CrossRef\]](#)
77. Barnwal, P.; Tiwari, G.N. Life cycle cost analysis of a hybrid photovoltaic/thermal greenhouse dryer. *Open Environ. Sci.* **2008**, *2*, 39–46. [\[CrossRef\]](#)
78. Vijayan, S.; Arjunan, T.V.; Kumar, A. Exergo-environmental analysis of an indirect forced convection solar dryer for drying bitter melon slices. *Renew. Energy* **2020**, *146*, 2210–2223. [\[CrossRef\]](#)
79. Shrivastava, V.; Kumar, A. Embodied energy analysis of the indirect solar drying unit. *Int. J. Ambient Energy* **2017**, *38*, 280–285. [\[CrossRef\]](#)

80. Espinosa, N.; Hösel, M.; Angmo, D.; Krebs, F.C. Solar cells with one-day energy payback for the factories of the future. *Energy Environ. Sci.* **2012**, *5*, 5117–5132. [[CrossRef](#)]
81. Prakash, O.; Kumar, A.; Kaviti, A.K.; Kumar, P.V. Prediction of the rate of moisture evaporation from jaggery in greenhouse drying using the fuzzy logic. *Heat Transf. Res.* **2016**, *46*, 923–935. [[CrossRef](#)]
82. Kumar, A.; Kandpal, T.C. Solar drying and CO₂ emissions mitigation: Potential for selected cash crops in India. *Sol. Energy* **2005**, *78*, 321–329. [[CrossRef](#)]
83. Aymen, E.L.; Hamdi, I.; Kooli, S.; Guizani, A. Drying of red pepper slices in a solar greenhouse dryer and under open sun: Experimental and mathematical investigations. *Innov. Food Sci. Emerg. Technol.* **2019**, *52*, 262–270. [[CrossRef](#)]
84. Singh, P.; Gaur, M.K. Review on development, recent advancement and applications of various types of solar dryers. *Energy Sources Part A Recovery Util. Environ. Eff.* **2020**, 1–21. [[CrossRef](#)]
85. Mishra, S.; Verma, S.; Chowdhury, S.; Dwivedi, G. Analysis of recent developments in greenhouse dryer on various parameters—a review. *Mater. Today Proc.* **2021**, *38*, 371–377. [[CrossRef](#)]
86. Khanlari, A.; Sözen, A.; Şirin, C.; Tuncer, A.D.; Gungor, A. Performance enhancement of a greenhouse dryer: Analysis of a cost-effective alternative solar air heater. *J. Clean. Prod.* **2020**, *251*, 119672. [[CrossRef](#)]
87. Choab, N.; Allouhi, A.; El Maakoul, A.; Kousksou, T.; Saadeddine, S.; Jamil, A. Review on greenhouse microclimate and application: Design parameters, thermal modeling and simulation, climate controlling technologies. *Sol. Energy* **2019**, *191*, 109–137. [[CrossRef](#)]
88. Mathioulakis, E.; Karathanos, V.T.; Belessiotis, V.G. Simulation of air movement in a dryer by computational fluid dynamics: Application for the drying of fruits. *J. Food Eng.* **1998**, *36*, 183–200. [[CrossRef](#)]
89. Bartzanas, T.B.T.K.C.; Boulard, T.; Kittas, C. Effect of vent arrangement on windward ventilation of a tunnel greenhouse. *Biosyst. Eng.* **2004**, *88*, 479–490. [[CrossRef](#)]
90. Prakash, O.; Kumar, A. ANFIS modelling of a natural convection greenhouse drying system for jaggery: An experimental validation. *Int. J. Sustain. Energy* **2014**, *33*, 316–335. [[CrossRef](#)]
91. Amjad, W.; Gilani, G.A.; Munir, A.; Asghar, F.; Ali, A.; Waseem, M. Energetic and exergetic thermal analysis of an inline-airflow solar hybrid dryer. *Appl. Therm. Eng.* **2019**, *166*, 114632. [[CrossRef](#)]
92. Jain, D.; Tiwari, G.N. Effect of greenhouse on crop drying under natural and forced convection I: Evaluation of convective mass transfer coefficient. *Energy Convers. Manag.* **2004**, *45*, 765–783. [[CrossRef](#)]
93. Krawczyk, P.; Badyda, K. Two-dimensional CFD modeling of the heat and mass transfer process during sewage sludge drying in a solar dryer. *Arch. Thermodyn.* **2011**, *32*, 3–16. [[CrossRef](#)]
94. Janjai, S. A greenhouse type solar dryer for small-scale dried food industries: Development and dissemination. *Int. J. Energy Environ.* **2012**, *3*, 383–398.
95. Prakash, O.; Kumar, A. ANFIS prediction model of a modified active greenhouse dryer in no-load conditions in the month of January. *Int. J. Adv. Comput. Res.* **2013**, *3*, 220.
96. Tanwanichkul, B.; Thepa, S.; Rordprapat, W. Thermal modeling of the forced convection Sandwich Greenhouse drying system for rubber sheets. *Energy Convers. Manag.* **2013**, *74*, 511–523. [[CrossRef](#)]
97. Prakash, O.; Kumar, A. Performance evaluation of greenhouse dryer with opaque north wall. *Heat Mass Transf.* **2014**, *50*, 493–500. [[CrossRef](#)]
98. Phusampao, C.; Nilnont, W.; Janjai, S. Performance of a greenhouse solar dryer for drying macadamia nuts. In Proceedings of the 2014 International Conference and Utility Exhibition on Green Energy for Sustainable Development (ICUE), Pattaya City, Thailand, 19–21 March 2014; pp. 1–5.
99. Romero, V.; Cerezo, E.; Garcia, M.; Sanchez, M. Simulation and Validation of Vanilla Drying Process in an Indirect Solar Dryer Prototype Using CFD Fluent Program. *Energy Procedia* **2014**, *57*, 1651–1658. [[CrossRef](#)]
100. Vintilă, M.; Ghiauş, A.G.; Fătu, V. Prediction of air flow and temperature profiles inside convective solar dryer. *Bull. UASVM Food Sci. Technol.* **2014**, *71*, 188–194. [[CrossRef](#)]
101. Sethi, V.; Arora, S. Improvement in greenhouse solar drying using inclined north wall reflection. *Sol. Energy* **2009**, *83*, 1472–1484. [[CrossRef](#)]
102. Morad, M.; El-Shazly, M.; Wasfy, K.; El-Maghawry, H.A. Thermal analysis and performance evaluation of a solar tunnel greenhouse dryer for drying peppermint plants. *Renew. Energy* **2017**, *101*, 992–1004. [[CrossRef](#)]
103. Baniasadi, E.; Ranjbar, S.; Boostanipour, O. Experimental investigation of the performance of a mixed-mode solar dryer with thermal energy storage. *Renew. Energy* **2017**, *112*, 143–150. [[CrossRef](#)]
104. Tiwari, S.; Tiwari, G.N.; Al-Helal, I.M. Performance analysis of photovoltaic–thermal (PVT) mixed mode greenhouse solar dryer. *Sol. Energy* **2016**, *133*, 421–428. [[CrossRef](#)]
105. Perea-Moreno, A.J.; Juaidi, A.; Manzano-Agugliaro, F. Solar greenhouse dryer system for wood chips improvement as biofuel. *J. Clean. Prod.* **2016**, *135*, 1233–1241. [[CrossRef](#)]
106. Tham, T.C.; Ng, M.X.; Gan, S.H.; Chua, L.S.; Aziz, R.; Chuah, L.A.; Hii, C.L.; Ong, S.P.; Chin, N.L.; Law, C.L. Effect of ambient conditions on drying of herbs in solar greenhouse dryer with integrated heat pump. *Dry. Technol.* **2017**, *35*, 1721–1732. [[CrossRef](#)]
107. Janjai, S.; Tohsing, K.; Lamlert, N.; Mundpookhier, T.; Chanalert, W.; Bala, B.K. Experimental performance and artificial neural network modeling of solar drying of litchi in the parabolic greenhouse dryer. *J. Renew. Energy Smart Grid Technol.* **2018**, *13*, 83–95.

108. Huddar, V.B.; Kamoji, M.A. Experimental investigation on performance of small passive solar greenhouse dryer for cashew kernel drying. *AIP Conf. Proc.* **2019**, *2080*, 030001.
109. Ferreira, A.G.; Charbel, A.L.T.; Pires, R.L.; Silva, J.G.; Maia, C.B. Experimental analysis of a hybrid dryer. *Exp. Anal. A Hybrid Dry.* **2007**, *6*, 3–7. [[CrossRef](#)]
110. Tuncer, A.D.; Sözen, A.; Khanlari, A.; Amini, A.; Şirin, C. Thermal performance analysis of a quadruple-pass solar air collector assisted pilot-scale greenhouse dryer. *Sol. Energy* **2020**, *203*, 304–316. [[CrossRef](#)]
111. Amer, B.; Hossain, M.; Gottschalk, K. Design and performance evaluation of a new hybrid solar dryer for banana. *Energy Convers. Manag.* **2010**, *51*, 813–820. [[CrossRef](#)]
112. Barnwal, P.; Tiwari, G.N. Experimental validation of hybrid photovoltaic-thermal (PV/T) greenhouse dryer under forced mode. *Int. J. Food Eng.* **2011**, *6*. [[CrossRef](#)]
113. Okoroigwe, E.C.; Ndu, E.C. Comparative evaluation of the performance of an improved solar-biomass hybrid dryer. *J. Energy S. Afr.* **2017**, *26*, 38. [[CrossRef](#)]
114. Reyes, A.; Mahn, A.; Huenulaf, P.; González, T. Tomato dehydration in a hybrid-solar dryer. *J. Chem. Eng. Process Technol.* **2014**, *5*, 1–8.
115. Aritesty, E.; Wulandani, D. Performance of the Rack Type-greenhouse Effect Solar Dryer for Wild Ginger (*Curcuma xanthorrhiza* Roxb.) Drying. *Energy Procedia* **2014**, *47*, 94–100. [[CrossRef](#)]
116. Sajith, K.G.; Muraleedharan, C. Economic analysis of a hybrid photovoltaic/thermal solar dryer for drying amla. *Int. J. Eng. Res. Technol. IJERT* **2014**, *3*, 907–910.
117. Dhanushkodi, S.; Wilson, V.H.; Sudhakar, K. Thermal Performance evaluation of Indirect forced cabinet solar dryer for cashew drying. *Am.-Eurasian J. Agric. Environ. Sci.* **2014**, *14*, 1248–1254.
118. Vengsungnl, P.; Jongpluempiti, J.; Srichat, A.; Wiriyasart, S.; Naphon, P. Thermal performance of the photovoltaic-ventilated mixed mode greenhouse solar dryer with automatic closed loop control for Ganoderma drying. *Case Stud. Therm. Eng.* **2020**, *21*, 100659. [[CrossRef](#)]
119. Bassey, M.W. Design and performance of a hybrid crop dryer using solar energy and sawdust. In *Intersol Eighty Five*; Pergamon: Oxford, UK, 1986; pp. 1038–1042.
120. Nandwani, S.S. Design, construction and study of a hybrid solar food processor in the climate of Costa Rica. *Renew. Energy* **2007**, *32*, 427–441. [[CrossRef](#)]
121. Boughali, S.; Benmoussa, H.; Bouchekima, B.; Mennouche, D.; Bouguettaia, H.; Bechki, D. Crop drying by indirect active hybrid solar-Electrical dryer in the eastern Algerian Septentrional Sahara. *Sol. Energy* **2009**, *83*, 2223–2232. [[CrossRef](#)]
122. Reyes, A.; Mahn, A.; Cubillos, F.; Huenulaf, P. Mushroom dehydration in a hybrid-solar dryer. *Energy Convers. Manag.* **2013**, *70*, 31–39. [[CrossRef](#)]
123. Yassen, T.A.; Al-Kayiem, H.H. Experimental investigation and evaluation of hybrid solar/thermal dryer combined with supplementary recovery dryer. *Sol. Energy* **2016**, *134*, 284–293. [[CrossRef](#)]
124. Eltawil, M.A.; Azam, M.M.; Alghannam, A.O. Energy analysis of hybrid solar tunnel dryer with PV system and solar collector for drying mint (*Mentha Viridis*). *J. Clean. Prod.* **2018**, *181*, 352–364. [[CrossRef](#)]
125. Amer, B.M.; Gottschalk, K.; Hossain, M.A. Integrated hybrid solar drying system and its drying kinetics of chamomile. *Renew. Energy* **2018**, *121*, 539–547. [[CrossRef](#)]
126. Poonia, S.; Singh, A.K.; Jain, D. Design development and performance evaluation of photovoltaic/thermal (PV/T) hybrid solar dryer for drying of ber (*Zizyphus mauritiana*) fruit. *Cogent Eng.* **2018**, *5*, 1507084. [[CrossRef](#)]
127. Hao, W.; Liu, S.; Mi, B.; Lai, Y. Mathematical Modeling and Performance Analysis of a New Hybrid Solar Dryer of Lemon Slices for Controlling Drying Temperature. *Energies* **2020**, *13*, 350. [[CrossRef](#)]
128. Ayyappan, S. Performance and CO₂ mitigation analysis of a solar greenhouse dryer for coconut drying. *Energy Environ.* **2018**, *29*, 1482–1494. [[CrossRef](#)]
129. Motevali, A.; Koloor, R.T. A comparison between pollutants and greenhouse gas emissions from operation of different dryers based on energy consumption of power plants. *J. Clean. Prod.* **2017**, *154*, 445–461. [[CrossRef](#)]
130. Saini, V.; Tiwari, S.; Tiwari, G. Environ economic analysis of various types of photovoltaic technologies integrated with greenhouse solar drying system. *J. Clean. Prod.* **2017**, *156*, 30–40. [[CrossRef](#)]
131. Nayak, S.; Kumar, A.; Mishra, J.; Tiwari, G.N. Drying and Testing of Mint (*Mentha piperita*) by a Hybrid Photovoltaic-Thermal (PVT)-Based Greenhouse Dryer. *Dry. Technol.* **2011**, *29*, 1002–1009. [[CrossRef](#)]
132. Zhong, C.; Li, H.; Zhou, Y.; Lv, Y.; Chen, J.; Li, Y. Virtual synchronous generator of PV generation without energy storage for frequency support in autonomous microgrid. *Int. J. Electr. Power Energy Syst.* **2022**, *134*, 107343. [[CrossRef](#)]
133. Ren, L.; Kong, F.; Wang, X.; Song, Y.; Li, X.; Zhang, F.; Wang, J. Triggering ambient polymer-based Li-O₂ battery via photo-electro-thermal synergy. *Nano Energy* **2022**, *98*, 107248. [[CrossRef](#)]
134. Barnwal, P.; Tiwari, G.N. Grape drying by using hybrid photovoltaic-thermal (PV/T) greenhouse dryer: An experimental study. *Sol. Energy* **2008**, *82*, 1131–1144. [[CrossRef](#)]
135. Gong, X.; Wang, L.; Mou, Y.; Wang, H.; Wei, X.; Zheng, W.; Yin, L. Improved Four-channel PBTDPA Control Strategy Using Force Feedback Bilateral Teleoperation System. *Int. J. Control* **2022**, *20*, 1002–1017. [[CrossRef](#)]
136. Ban, Y.; Liu, M.; Wu, P.; Yang, B.; Liu, S.; Yin, L.; Zheng, W. Depth Estimation Method for Monocular Camera Defocus Images in Microscopic Scenes. *Electronics* **2022**, *11*, 2012. [[CrossRef](#)]

137. Cui, W.; Li, X.; Li, X.; Si, T.; Lu, L.; Ma, T.; Wang, Q. Thermal performance of modified melamine foam/graphene/paraffin wax composite phase change materials for solar-thermal energy conversion and storage. *J. Clean. Prod.* **2022**, *367*, 133031. [[CrossRef](#)]
138. Khadraoui, A.; Bouadila, S. Experimental and Economic Performance of Two Solar Dryer Systems in Tunisia. In *Low Carbon Energy Supply Technologies and Systems*; CRC Press: Boca Raton, FL, USA, 2020; pp. 41–60.
139. Guo, Z.; Tian, X.; Wu, Z.; Yang, J.; Wang, Q. Heat transfer of granular flow around aligned tube bank in moving bed: Experimental study and theoretical prediction by thermal resistance model. *Energy Convers. Manag.* **2022**, *257*, 115435. [[CrossRef](#)]
140. Chauhan, P.S.; Kumar, A.; Nuntadusit, C. Thermo-environmental and drying kinetics of bitter melon flakes drying under north wall insulated greenhouse dryer. *Sol. Energy* **2018**, *162*, 205–216. [[CrossRef](#)]
141. Chang, H.; Han, Z.; Li, X.; Ma, T.; Wang, Q. Experimental study on heat transfer performance of sCO₂ near pseudo-critical point in airfoil-fin PCHE from viewpoint of average thermal-resistance ratio. *Int. J. Heat Mass Transf.* **2022**, *196*, 123257. [[CrossRef](#)]